Accepted Manuscript

Fused and unzipped carbon nanotubes, electrochemically treated, for selective determination of dopamine and serotonin

M. Celina Bonetto, Fernando F. Muñoz, Virginia E. Diz, Natalia J. Sacco, Eduardo Cortón

PII: S0013-4686(18)31467-1

DOI: 10.1016/j.electacta.2018.06.179

Reference: EA 32172

To appear in: *Electrochimica Acta*

Received Date: 16 February 2018

Revised Date: 26 June 2018

Accepted Date: 26 June 2018

Please cite this article as: M.C. Bonetto, F.F. Muñoz, V.E. Diz, N.J. Sacco, E. Cortón, Fused and unzipped carbon nanotubes, electrochemically treated, for selective determination of dopamine and serotonin, *Electrochimica Acta* (2018), doi: 10.1016/j.electacta.2018.06.179.

GC modified electrodes

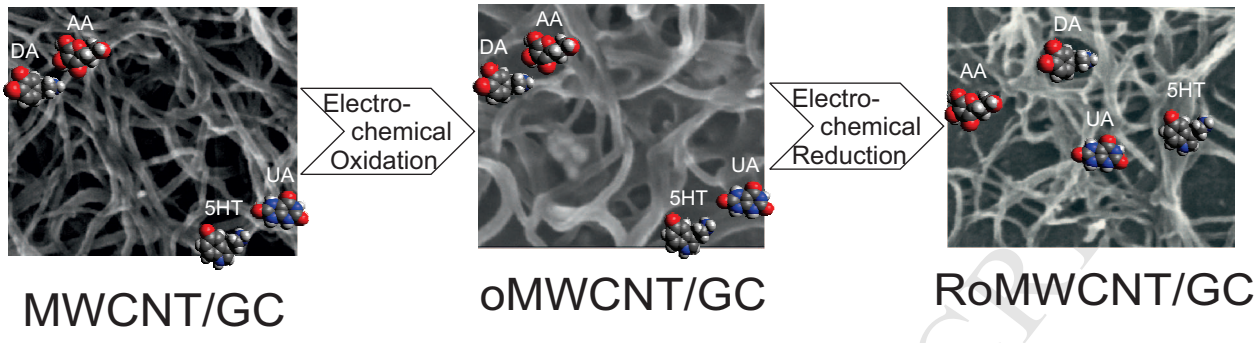

MWCNT/GC oMWCNT/GC RoMWCNT/GC

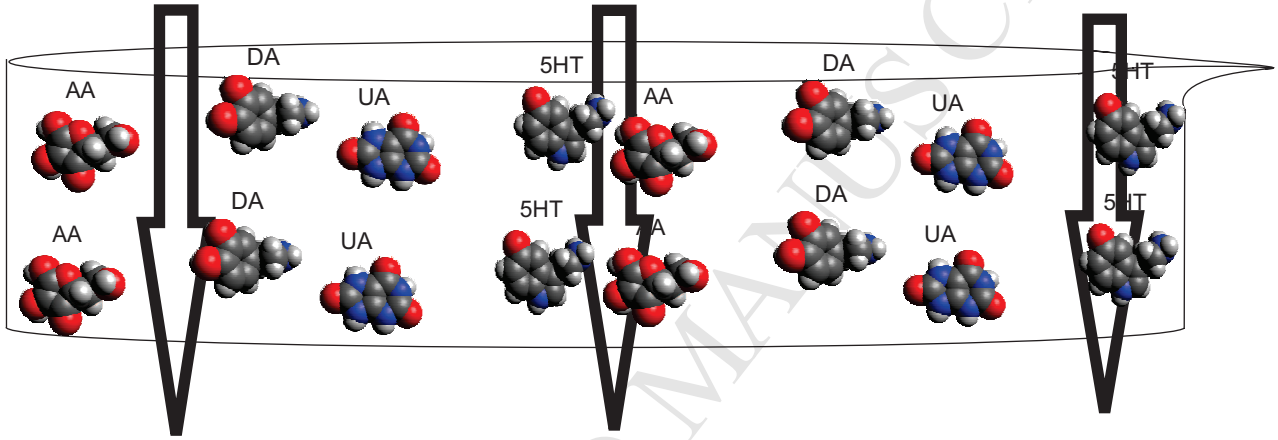

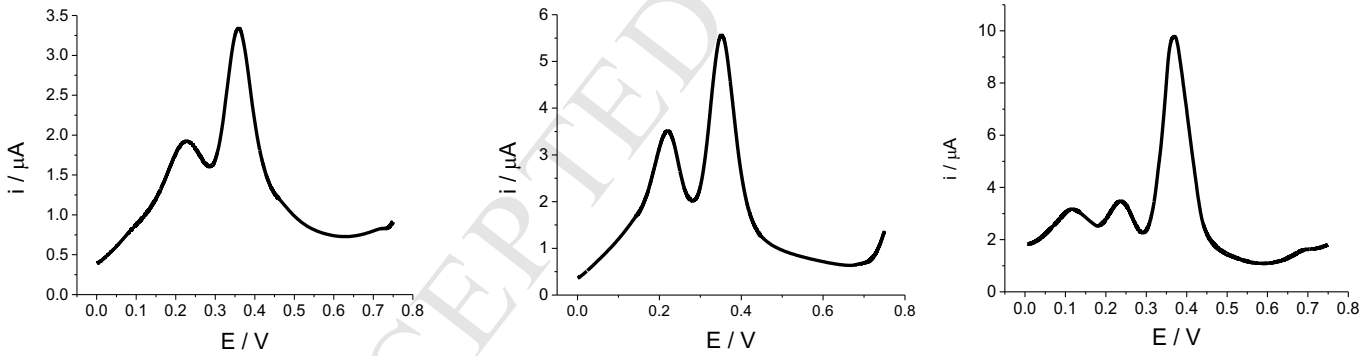

Fused and unzipped carbon nanotubes, electrochemically treated, for selective determination of dopamine and serotonin

M. Celina Bonetto[1*], Fernando F. Muñoz[3,4], Virginia E. Diz[2], Natalia J. Sacco[1], Eduardo Cortón[1]

[1]Laboratory of Biosensors and Bioanalysis (LABB), Departamento de Química Biológica e IQUIBICEN-CONICET, Intendente Güiraldes 2160, Pabellón 2, Ciudad Universitaria, Facultad de Ciencias Exactas y Naturales, Universidad de Buenos Aires. Ciudad Autónoma de Buenos Aires C1428EGA, Argentina

[2]Departamento de Química Inorgánica, Analítica y Química Física, Intendente Güiraldes 2160, Pabellón 2, Ciudad Universitaria, Facultad de Ciencias Exactas y Naturales, Universidad de Buenos Aires. C1428EGA. Ciudad Autónoma de Buenos Aires, Argentina

[3]DEINSO (Departamento de Investigaciones en Sólidos), UNIDEF-CITEDEF, J.B. de la Salle 4397, (1603) Villa Martelli, Buenos Aires, Argentina

[4]CONICET, Buenos Aires, Argentina

Abstract

Glassy carbon electrodes (GC) were modified with multiwalled carbon nanotubes (MWCNT/GC) and electrochemically treated first by applying an oxidation potential and then a reduction potential. The resulting electrodes were characterized via scanning electron microscopy, Raman spectroscopy, energy dispersive spectroscopy, and electrochemical techniques, particularly cyclic voltammetry using the redox probes $Fe(CN)_6^{3-/4-}$ and $Ru(NH_3)^{2+/3+}$ and electrochemical impedance spectroscopy using $Fe(CN)_6^{3-/4-}$. These modified electrodes showed an electrochemical determination selective for dopamine (DA)

* Corresponding author. Tel.: (++54 +11) 4576-3300

E-mail: celinatt@yahoo.com.ar or mcbonetto@qb.fcen.uba.ar (M. Celina Bonetto)

and serotonin (5HT) in the presence of ascorbic acid (AA) and uric acid (UA), simultaneously measured, with a high reproducibility (an RSD of 1.7% for DA and 1.6% for 5HT) and a limit of detection (LOD) of 235 nmol L^{-1} for DA and 460 nmol L^{-1} for 5HT. The GC electrodes modified with oxidized MWCNT, subsequently reduced, showed higher selectivity towards the oxidation of DA and 5HT compared with GC bare electrodes or modified with MWCNT or oxidized MWCNT.

Keywords: multiwalled carbon nanotubes; electrochemical treatment; hybrid film; dopamine; serotonin

1. Introduction

The production of electrodes for electrochemical devices require certain characteristics such as high electrical conductivity, mechanical and chemical stability, large surface area and a reasonable cost of their mass production. Hence carbon nanotubes and graphene are some of the carbon allotropes most intensively explored in materials science for disposable electrodes development for the determination of biomolecules [1-3].

Graphene is a single atom thick, a 2D sheet of sp^2 hybridized carbon atoms (double-bonded), densely packed in a honeycomb crystal lattice. Due to its structure, graphene has all of its atoms on the surface, which gives it an excellent biosensing potential in the nanoscale [4].

The most important property of graphene is its excellent electrical conductivity; electronically, graphene is a semiconductor with zero bandgap [5,6]. Any modification in the crystal lattice will alter the graphene band structure. Particularly, a variation of the

hybridization state of carbon atoms [7], other atoms or molecules incorporated in the lattice, and/or defects on graphene [8] can directly influence in the electrical properties of graphene. Similarly, the introduction of strong edge states and quantum confinement via structural constraints (nanoribbons, quantum dots, nanomesh) will have the same effect [9].

The methods currently in use to obtain near-perfect graphene sheets are expensive and/or time consuming. To overcome these difficulties, a number of methods such as the one proposed by Hummer and its modifications have been reported and involve less time and effort [10]. Several of these methods involve first an oxidation step, followed by a reduction step, to provide a better yield of material at the cost of lattice imperfections; hence, the materials as obtained are referred as "graphene-like". The oxidation step is absolutely necessary, since it provides individual layers of graphene oxide (GO) that will turn into graphene after reduction [11].

Conductivity of GO depends on the extent of oxidation. During oxidation treatment the sp^2 carbons are being continuously modified, with oxygen functionalities, to sp^3 carbons. The reduction of this GO partially restores the sp^2 hybridization, improving the conductive behaviour and yielding a graphene-like material [6]. Carbon nanotubes present the structure of a sheet of graphene rolled into a well-ordered tube. Hence, an alternative way to obtain a graphene-like material consists of unzipping a carbon nanotube.

One of the more successful approaches to convert carbon nanotubes (CNTs) into graphene nanoribbons (GNR) is Kosynkin/Tour´s longitudinal unzipping, using a mixture of potassium permanganate and concentrated sulfuric acid [12]. However, this method has several problems, primarily related to the use of strong oxidizing agents that will create

defect sites which could hamper the electronic properties of graphene and diminish electron mobility and conductivity, along with waste disposal conditions and the possibility of evolution of explosive gases [13].

Shinde et al. (2011) have reported an electrochemical approach to transform MWCNTs to reduced GNRs (rGNRs) under ambient conditions simplifying experimental and waste disposal conditions [14]. This approach has not been used, to our knowledge, in the design of electrochemical sensors for the determination of dopamine (DA) and serotonin (5HT), and seemed a good choice given the mechanical and chemical stability of rGNR, the low-cost production of the modified electrodes and their large surface area.

Electrochemical determination of DA and 5HT is of great interest for identification of cognitive dysfunctions in neurological diseases such as depression, Parkinson, epilepsy, squizofrenia, or senile dementia as early as possible to minimize the deleterious effects and production losses by young disabled population [15-18]. The ability to monitor physiological changes in levels of DA and 5HT could also benefit the design of better therapeutics and the evaluation of their efficacy towards those neurological disorders.

Due to the redox behaviour of DA and 5HT, the electrochemical methods are suitable for their analytical determinations. However, there are electroactive interferences for electrochemical measurements such as ascorbic acid (AA) and uric acid (UA) that present an overlapping of their anodic peak potentials, between 0.2 and 0.35 V, with a paste carbon electrode [19-23].

DA, UA and AA have been simultaneously determined using electrodes modified with: graphene oxide electrochemically reduced [24], pristine graphene [25], reduced graphene

oxide with Pt nanoparticles [23], or GO-porphyrin electrochemically reduced [17]. There are few reports in literature about simultaneous determination of DA, 5HT and AA [26]. There are works that determine DA, AA, UA, and tryptophan simultaneously [27-29] nonetheless, it is still an issue the determination of DA and 5HT simultaneously in the presence of UA and AA using only carbon-based electrodes. A recent work has determined DA with a high sensibility (1nM) even though in this work DA is measured in different concentrations only in presence of AA [30].

In this work we report the fabrication and characterization of modified electrodes MWCNT/GC electrochemically treated, based on the approach presented by Shinde et al. to produce rGNR [14], and its application to the simultaneous determination of DA and 5HT in the presence of AA and UA.

The physicochemical properties of the fabricated sensors were studied by scanning electron microscopy (SEM), Raman spectroscopy, energy dispersive X-ray spectroscopy (EDS), and their electrochemical performance was studied by cyclic voltammetry (CV) and electrochemical impedance spectroscopy (EIS). For the electrochemical characterization, we used the inner-sphere redox probe Fe $(CN)_6^{3-/4-}$ and the outer-sphere redox probe $Ru(NH_3)_6^{2+/3+}$. Electrode kinetic parameters have been determined by the Tafel equation in order to prove theoretically the obtained results in the CV and DPV studies (calibration curves with the four compounds).

Based on these characterizations, the obtained electrodes were called RoMWCNT/GC, rather than rGNR/GC, because they present a hybrid film of MWCNT fused and unzipped

near the GC electrode surface. In the interface electrode/solution of the electrodes, we could see MWCNT similar to those present in the electrodes without treatment.

To our best knowledge this is the first time that a carbon electrode with graphene-like characteristics (RoMWCNT/GC) exhibited excellent electrochemical performance with good reproducibility for the determination of DA and 5HT. The results obtained clearly show that the electrochemical treatment of MWCNT/GC (an oxidation and then a reduction) improves the selective determination of DA and 5HT in presence of UA and AA.

2. Experimental

2.1. Reagents and instrumentation

Potassium phosphate monobasic (KH_2PO_4), potassium phosphate dibasic (K_2HPO_4), potassium ferrocyanide/ferricyanide ($Fe(CN)_6^{3-/4-}$), potassium chloride (KCl), potassium sulphate (K_2SO_4), sodium sulphate (Na_2SO_4), sulfuric acid (H_2SO_4), absolute ethanol, L-ascorbic acid, and uric acid of analytical grade were used as received.

MWCNTs (> 98% carbon basis, 10 nm outer diameter, 4.5 nm inner diameter and 3.5 μm lenght), DA (3-hydroxytyramine hydrochloride) and 5HT (5-hidroxytryptamine hydrochloride) and hexaammine-ruthenium (III) chloride ($[Ru(NH_3)_6]Cl_3$) (96%) were obtained from Sigma Aldrich.

Phosphate buffered saline solution (PBS) was prepared using K_2HPO_4 and KH_2PO_4 (0.1 mol L^{-1}, pH = 7.0) with KCl 0.1 mol L^{-1} in milliQ water.

All the electrochemical measurements were made with a standard three-electrode system. A GC bare electrode (Structure Probe, Inc. PA, USA), or modified with MWCNT, oMWCNT or RoMWCNT, were assayed as working electrode. A Pt foil was used as counterelectrode. Two different reference electrodes were used, either Ag/Ag_2SO_{4sat} or $Ag/AgCl_{sat}$.

Electrochemical measurements were performed at room temperature (ca. 25 °C) in solutions deoxygenated with N_2 high purity (O_2 content < 0.01 ppm) for 40 min. Solutions were used freshly prepared in Milli-Q water.

Electrochemical measurements were done using a Potentiostat/Galvanostat/ZRA (Series G 300^{TM} and Interface 1000 from Gamry Instruments Inc. Warminster, USA).

Sonications were made using an ultrasonic bath (Cole-Parmer Instrument Company, LLC. IL, USA).

Scanning electron microscope (SEM) images were recorded on a SEM Carl Zeiss NTS SUPRA 40 (Carl Zeiss NTS GmbH, Oberkochen, Germany).

An Apollo X EDAX spectrophotometer (AMETEK, NJ, USA) was used for EDS measurements. Samples were bombarded with 25 kV electrons and the measuring time was 50 s.

Raman measurements were performed in a Confocal Horiba Jobin Yvon Dilor XY 800 (HORIBA, Ltd. Tokyo, Japan). A 514 nm line of a continuous wave Ar laser (13 mW) was used by means of a 100x working distance objective.

2.2. Electrochemical oxidation and reduction of MWCNT/GC in H_2SO_4 0.5 mol L^{-1}

The GC electrodes (1 mm diameter) were pretreated via a polishing with alumina powder on a wet cloth (0.3 μm), obtaining a mirror-like surface, and then washed with copious amounts of water. Afterwards the electrodes were sonicated for 5 min in milli-Q water and 5 min in ethanol and finally dried 15 min at 50 ºC. A dispersion of MWCNT (0.5 mg mL^{-1} of MWCNTs in absolute ethanol) was sonicated for 120 min. 5 μL of the dispersion was deposited onto a pretreated GC electrode, followed by drying at 50 ºC.

MWCNT/GC were treated first by applying a fixed oxidation potential of +0.72 V for 6 h in 0.5 mol L^{-1} H_2SO_4 continuously deoxygenated with N_2 to obtain oMWCNT/GC. In the second step of the electrochemical treatment oMWCNT/GC was treated by applying a fixed reduction potential of -0.75 V for 6 h in 0.5 mol L^{-1} H_2SO_4 continuously deoxygenated with N_2 to obtain RoMWCNT/GC.

CVs, performed in 0.5 mol L^{-1} H_2SO_4 at a scan rate of 100 mV s^{-1}, were made to study the modifications of the electrodes after 1, 2, 3, 4, 5, and 6 hours of applying the oxidation potential, between 0.1 and 1 V. Similarly, after 1, 3 and 5 h of applying the reduction potential, CVs were also performed, this time between -0.8 and 0 V.

An Ag/Ag_2SO_{4sat} was used as reference electrode for these electrochemical treatments of MWCNT/GC in H_2SO_4 to avoid the presence of Cl^- that may interfere in modified electrodes [31].

2.3. Electrochemical characterization of the electrodes

The electrochemical characterization of the GC, MWCNTs/GC, oMWCNT/GC and RoMWCNT/GC electrodes was made through CV and EIS techniques using a $Ag/AgCl_{sat}$ RE.

Electrochemical surface areas (ECSA) were calculated by CV of 5 mmol L^{-1} $Fe(CN)_6^{3-}$ in 1 mol L^{-1} KCl and performed by scanning the potential between -0.3 and 0.7 with a scan rate of 50 mV s^{-1}. CV were also performed in KCl 0.1 mol L^{-1} containing 1 mmol L^{-1} Ru $(NH_3)_6^{2+/3+}$ scanning the potential between -0.5 and 0.2 V with a scan rate of 50 mV s^{-1}.

CV measurements were performed in PBS containing 5 mmol L^{-1} $Fe(CN)_6^{3-/4-}$ scanning the potential between -0.3 and 0.7 V with a scan rate of 50 mV s^{-1}.

Electrochemical impedance spectroscopy (EIS) measurements were performed to a 5 mmol L^{-1} $Fe(CN)_6^{3-/4-}$ in PBS at 5 mV_{AC}, 0.24 V_{DC}, between 0.1 to 10^5 Hz, and 10 points/decade.

2.4. CV and DPV measurements of 5HT, AA, DA, and UA

Different concentrations of 5HT, AA, DA and UA were prepared in PBS. CVs were performed scanning the potential at a scan rate of 50 mV s^{-1}. DPV were performed scanning the potential with a pulse size of 50 mV, step size of 5 mV, sample period of 0.35 s and pulse time of 0.05 s. CV and DPV were made using a $Ag/AgCl_{sat}$ RE.

Graphical models of DA, 5HT, UA and AA that appears in the graphical abstract were made using Avogadro 1.2 [32]

3. Results and Discussion

3.1. SEM characterization

It can be seen in Fig. 1 SEM images of GC modified electrodes with MWCNT, oMWCNT, and RoMWCNT. In oMWCNT/GC and RoMWCNT/GC a mesh or matrix made with fused nanotubes and partially unzipped nanotubes can be seen (fused nanotubes circled in black and unzipped nanotubes circled in white).

In Fig.1d it can be seen a RoMWCNT/GC with a high density of MWCNTs with no differences to those MWCNTs without treatment (in Fig. 1a can be seen MWCNT/GC), and a little zone (squared in black) with apparently fused nanotubes in an inner layer. The zoom made in the squared region show clear differences in the morphology of the nanotubes near the GC surface (Figs. 1e and f). It has to be noted that the dispersion of MWCNT used to prepare the modified electrodes presented nanotubes without fusion and or unzipping, as those observed in the MWCNT/GC electrodes.

If we compare Fig. 1a with Figs. 1b and c it can be seen fused (circled in black) and unzipped nanotubes (circled in white) in MWCNT/GC after the electrochemical oxidation treatment. We can also see a significant difference in the width of the isolated nanotubes between oMWCNT/GC (Fig. 1c) and RoMWCNT/GC (Fig. 1f). The width of the CNT varies with oxygen content (present here as surface functionalities) then, the nanotubes in oMWCNT/GC will have wider diameters than their reduced counterparts (as in, surface functionalities free). In fact, the loss of width of the nanotubes after the reduction treatment is used by some authors as criteria for effective reduction [33].

Nanotubes fused and unzipped can be clearly seen in regions where a less concentration of MWCNT treated is present, nearby the GC surface. Shinde et al. [14] did not mentioned the fusion between nanotubes, but it should be noted that the nanotubes used in this work are

smaller than those used by Shinde (we used MWCNT of 10 nm diameter and Shinde has used MWCNT of approximately 100 nm diameter). This fact can be explained as follows: since the oxidation potential applied may lead to an increase of local temperature in some MWCNTs [34] and keeping in mind that this fact is probably magnified by the relatively large surface area of the MWCNTs, these combined factors probably lead to the fusion between nanotubes (apart from the unzipping) near the GC surface.

Thus, our modified electrodes present an inner layer with nanotubes fused and unzipped near the GC electrode surface, and an outer layer with MWCNTs mostly (Fig. 1d).

3.2. Raman spectroscopy analysis

Raman spectroscopy is a powerful tool and a non-destructive technique to distinguish between different types of ordered and disordered bonding environments of sp^2 and sp^3. In our electrodes, Raman spectroscopy revealed that the density of defects increased from MWCNT/GC to RoMWCNT/GC after the electrochemical treatments (oxidation and reduction) as shown in Fig. 2.

The intensity of the defects (sp^3) related peak at 1350 cm^{-1} (peak D) vs. the intensity of the peak related to sp^2 hybridization (characteristics of graphitic-like materials) at 1560 cm^{-1} (peak G) is a common tool among carbon based raman spectra to determine the graphene character. The ratio I_D/I_G increased from 1 to 1.3 after the electrochemical oxidation of MWCNT. The concomitant electrochemical reduction process lowers that ratio down to 1.2 for the RoMWCNT/GC electrode.

The ratio I_D/I_G increased upon oxidation of the MWCNT/GC owing to the unzipping of the carbon nanotubes, which generated a massive number of defects (increasing peak D) coupled with the oxygen functionalization, which decreases peak G due to the loss of graphitic characteristics.

It should be noted that the two processes are not necessarily coupled, nor the variations of the peaks are proportional [35], hence the decrease from 1.3 to 1.2 during reduction is an important criterion for the restitution of sp^2 features (there are evidences that graphene-like materials could have strong peaks D even after thorough reduction, since many defects do not disappear under reducing conditions) [33].

Additionally, despite the importance of the ratio I_D/I_G as a diagnostic tool, it must be kept in mind that the sharp peak 2D at 2700 cm^{-1} is only present in graphitic materials and is, at least, also a proof of graphene-like features [35]. In our case, peak 2D increases its intensity going from MWCNT to either their oxidized or reduced forms, which is a strong sign of graphitization, in very good agreement with the intended transformation to a graphene-like material. Thus, despite the semiconductive nature of our modified electrodes, RoMWCNT/GC would be expected to be more conductive than oMWCNT/GC, based on the lower ratio I_D/I_G that they present hence a good candidate for further characterizations.

3.3. EDS studies

EDS analysis was used to confirm the C/O ratio in different modified electrodes (Table 1). The EDS spectrum showed that the O element contained in oMWCNT/GC was (3.89 ± 0.18) at%, in accordance with results from Raman after that the electrochemical oxidation process generated oxygen functional groups. RoMWCNT/GC contained (2.05 ± 0.12) at%

of O element revealing a very high extent of reduction of those oxygen functional groups after the electrochemical reduction process. There were minimum differences between the at% of the O element contained in the MWCNT/GC (1.72 ± 0.21) at% from the one contained in the RoMWCNT/GC, but there were big differences in the images of SEM between both modified electrodes (Fig.1).

It should be noted that, the MWCNT dispersions used presented a 0.2 at% of the O element, therefore, it could be considered that the at % present in the MWCNT/GC and RoMWCNT comes from the GC electrode.

The ratio C/O is an additional, albeit complementary, tool used to monitor the extent of the process of graphitization [33]. In our case the ratio C/O of the oMWCNT/GC increased from 25:1 to 48:1 in the RoMWCNT/GC, confirming a high degree of reduction after the corresponding electrochemical step. This ratio increase is in good agreement with the change in the ratio I_D/I_G seen in the Raman results and the concept that the extent of reduction and restitution of the sp^2 hybridization does not mean that the defects generated in the oxidation step disappear after reduction.

3.4 Electrochemical oxidation of MWCNT/GC and reduction of oMWCNT/GC

In order to study the electrochemical oxidation of MWCNT/GC and reduction of oMWCNT/GC, we followed the process through cyclic voltammetry. We could see an oxidation peak approximately at 0.63 V that increased its height along with the oxidizing process of the MWCNTs (Fig. 3a). The presence of this peak, together with the increase in the D band in Raman spectra in comparison with the MWCNT/GC, and the EDS higher

content of O element in the oMWCNT/GC, strongly suggest that the MWCNTs are oxidized after applying a potential of 0.72 V for 6 h.

Fig. 3b shows that an increase in current (in absolute values) takes place as long as the reduction potential is being applied (in the range from 0 to -0.8 V). These moderately strong cathodic currents show an effective reduction, which is in accordance with the lower I_D/I_G ratio for the RoMWCNT/GC, as well as the high C/O ratio obtained by means of EDS.

3.5. Electrochemical studies using $Fe(CN)_6^{3-/4-}$ or $Ru(NH_3)_6^{2+/3+}$ redox probes

To study the electrochemical properties of GC, MWCNT/GC, oMWCNT/GC and RoMWCNT/GC, we used $Fe(CN)_6^{3-/4-}$ and $Ru(NH_3)_6^{2+/3+}$ as an inner-sphere and outer-sphere electron transfer redox probe respectively [36,37]. In both cases, smaller ΔE_p values are taken as a sign of increased reversibility and better electron transfer kinetics, since any change in the voltammetric response is ascribable to the nature of the electrode and not due to the redox probes involved, which are electrochemically reversible. This way, we purposely focus on the electrode much more than on the redox couple itself.

3.5.1 Inner-sphere electrochemical characterization

Fig. 4a shows the CV of $Fe(CN)_6^{3-/4-}$ in PBS at GC, MWCNT/GC, oMWCNT/GC and RoMWCNT/GC electrodes. A higher ΔE_p is seen with the RoMWCNT/GC electrode when comparing with the GC electrode, which could be seen as a significant decrease in reversibility. It should be noted that RoMWCNT/GC presented a lower ΔE_p value than

oMWCNT/GC (Table 2 and Fig. 4a), which means that the reduced modified electrode still shows increased reversibility.

Being a classical example of an inner-sphere electrode reaction, $Fe(CN)_6^{3-/4-}$ is known to have a surface-sensitive response, which can be ascribed to the increase in ΔE_p values going from naked GC electrodes to the MWCNT activated ones. The next section will further explore this idea complementing it with an outer-sphere redox probe.

The values of electrochemical surface area (ECSA) of GC, MWCNTs/GC, oMWCNT/GC and RoMWCNT/GC were calculated based on the Randles-Sevcik equation (1), assuming mass transport only by diffusion process (i.e reversible process, hence the utilization of the $Fe(CN)_6^{3-/4-}$ couple) (Table 2) [38,39].

$$Ip = 0.4463\, A\, c\, \gamma^{1/2}\, D^{1/2}\, RT^{-1/2}\, n^{3/2}\, F^{3/2} \quad (1)$$

where n is the number of electrons participating in the reaction, A is the electroactive surface area, D is the diffusion coefficient of the molecule ($6.7 \pm 0.02\ 10^{-6}$ $cm^2\ s^{-1}$), c is the analyte concentration (mol cm^{-3}), and γ is the scan rate (V s^{-1}). Table 2 shows that the values of ECSA are approximately one order of magnitude after the GC electrode were modified with MWCNT and further electrochemical treatments were applied.

EIS was chosen to further characterize the modification process of GC electrodes and their capacity of electron transfer, once again using $Fe(CN)_6^{3-/4-}$.

The Nyquist plots for all the electrodes are presented in Fig. 4b. It can be seen that when the electrodes are activated by plain or modified MWCNT deposition a huge improvement takes place. Also, the RoMWCNT showed a better response. The higher electrocatalytic

performance of RoMWCNT/GC was confirmed by the reduction of charge transfer resistance (R_{CT}), the semicircle diameter in the Nyquist plot (the inset in Fig. 4b shows that the semicircle is practically absent for RoMWCNT/GC, which is a strong indicator that only mass transfer effects are present, which in this context implies the better electrocatalytic activity for this redox couple).

The values of R_{CT}, determined by fitting the data using an appropriate equivalent circuit, are shown in Table 2. This data demonstrates the enhancement of electron transfer rate for redox species Fe $(CN)_6^{3-/4-}$ at RoMWCNT/GC. It should be noted that despite the ECSA of MWCNT/GC, oMWCNT/GC or RoMWCNT/GC are similar, R_{CT} values for the RoMWCNT/GC are half the R_{CT} values of MWCNT/GC and almost 4 times lower from the values of oMWCNT/GC. Furthermore, RoMWCNT/GC presents lower RSD values demonstrating the reproducibility of the electrochemical treatments and stability of the electrochemical properties of these electrodes.

3.5.2 Outer-sphere electrochemical characterization

In the prior section, we proposed the idea of an activated RoMWCNT/GC, precisely due to the reduction process itself, evaluated with the typical $Fe(CN)_6^{3-/4-}$ inner-sphere redox probe. In order to add further analysis to this idea, it is necessary to evaluate the electrode response with an outer-sphere redox probe, eliminating any interference due to surface-sensitive processes. Precisely, since this probe is ideally independent of surface related mechanisms, one can ascribe the observed differences between electrodes, entirely to the electrochemical treatments administered upon them.

Fig. 4c shows the CV of $Ru(NH_3)_6^{2+/3+}$ in KCl at GC, MWCNT/GC, oMWCNT/GC and RoMWCNT/GC electrodes. It can be clearly seen that the ΔE_p values show better responses going from bare GC to modified GC electrodes. More importantly, ΔE_p decreases going from oMWCNT/GC to RoMWCNT/GC, which means better reversibility and thus better electrochemical activation.

The use of $Ru(NH_3)_6^{2+/3+}$ allows to better display the improved behavior given by the treatment of the modified electrodes itself, which can be seen in the values of ΔE_p almost constant between the of MWCNT/GC, oMWCNT/GC and RoMWCNT/GC, since all of those values approach fairly well the theoretical ΔE_p value of 59 mV, typical for a reversible couple. With $Fe(CN)_6^{3-/4-}$ all the results of ΔE_p obtained with this redox probe are much higher than the theoretical 59 mV value, proving the importance of the use of an outer-sphere probe, since it provided clear evidence of a true reversible behavior for the electrode processes once they have been activated by the addition of MWCNT.

To further evaluate the impact of the usage of an outer-sphere probe, the values of ECSA were calculated for all the electrodes, once again based on the Randles-Sevcik equation, using D as the diffusion coefficient of the $Ru(NH_3)_6^{3+}$ molecule ($9.1\ 10^{-6}$ cm^2 s^{-1} in 0.1 mol L^{-1} KCl supporting electrolyte) [40].

The values of ECSA obtained with both redox probes were different; althought in one key aspect, the relation between them was alike: using either $Fe(CN)_6^{3-/4-}$ or $Ru(NH_3)_6^{2+/3+}$ the values of ECSA were approximately one order of magnitude higher after the GC electrode were modified with MWCNT and further electrochemical treatments were applied, showing the importance of the activation process.

It is important to notice that the $Ru(NH_3)_6^{2+/3+}$ case provide the values of ECSA which present only small variations once the GC electrode have been modified by MWCNT, in agreement with the narrow ΔE_p values so obtained, so the outer-sphere probe points toward a true reversible process taking place in the electrode surface. This fact could never be pointed out based in the inner-sphere probe results alone.

The effective heterogeneous electron transfer (HET) rate constant, $k°_{eff}$, was determined utilizing a method developed by Nicholson [41], applicable for quasi-reversible systems, and calculated for each modified electrode, plotting ψ against $[\pi D n \nu F/(RT)]^{-1/2}$ as suggested by Brownson et al. [40] where ψ is a kinetic parameter, D is the diffusion coefficient for $Ru(NH_3)_6^{3+}$, n is the number of electrons involved in the process, F is the Faraday constant, R the gas constant, T the temperature, and n the scan rate used (we used a range between 0.025 and 0.15 V).

The kinetic parameter ψ was calculated following equation (2)

$$\psi = (-0.6288+0.0021\ X) / (1-0.017\ X) \quad (2)$$

X being ΔE_p.

The $k°_{eff}$ calculated for bare GC was $3.17\ 10^{-2}$, this value is in agreement with Brownson´s result for GC [40]. Our modified electrodes presented $k°_{eff}$ of $3.2\ 10^{-1}$, $5.54\ 10^{-2}$, $4.51\ 10^{-2}$ for RoMWCNT/GC, oMWCNT/GC, and MWCNT/GC, respectively. These values are higher than those calculated by Brownson with the EPPG electrode, therefore these results, coupled with the structural differences seen in Raman and EDS studies discussed previously for RoMWCNT/GC, as well as the changes in EIS after the electrochemical process indicating that RoMWCNT/GC presents an improved conductivity (Table 2 and

section 3.5.1) and the value of ΔE_p of 60 mV using $Ru(NH_3)_6^{2+/3+}$, are strong evidence that these modified electrodes exhibit favorable electrochemical properties to be explored with biological molecules.

3.6. Electrochemical measurements of AA, DA, UA and 5HT and kinetic analysis of the modified electrodes

We have studied the electrochemical behaviour of modified electrodes obtained by following the protocol stated by Shinde [14]. CV measurements were made in samples containing 5HT, AA, DA, and UA, employing either a GC, MWCNT/GC, oMWCNT/GC or RoMWCNT/GC electrodes. As expected and in agreement with previously published work, Fig. 5 show that the four compounds of the mixture were not identified using GC, MWCNT/GC, or oMWCNT/GC.

At bare GC electrodes only one clear anodic peak was obtained near 415 mV (inset in Fig. 5). With MWCNT/GC and oMWCNT/GC two defined peaks were found when different concentrations of 5HT, AA, DA, and UA were assayed (Fig. 5). The peaks were found almost at the same potentials with both electrodes (250.8 ± 18 mV and 367 ± 30 mV, n=3) and higher currents were obtained with oMWCNT/GC. It can be seen that there is a significant improvement in the signals going from bare GC electrodes to the modified ones, a fact that is in accordance with the evidence of electrode activation mentioned in the above sections. Nevertheless, it is clear that these three electrodes presented poor selectivity and sensitivity.

In contrast, four well-defined peaks of oxidation, corresponding to AA, DA, UA and 5HT from left to right, were observed using the RoMWCNT/GC electrode in samples with different concentrations of AA, DA, UA and 5HT (inset Fig. 6a). The peaks of oxidation found were (101 ± 24) mV for AA, (233 ± 4) mV for DA, (363 ± 10) mV for UA and (683 ± 11) mV for 5H; with an RSD of 1.7% for DA and 1.6% for 5HT (values of SD were calculated using three different electrodes, n=3).

The presence of noticeable peaks in the reverse cathodic region of any of these four biological compounds (but much weaker than those from the anodic region) are an indication of a kinetic moderately favorable, clearly not irreversible, but also not fully reversible. These biological molecules show slow to moderate kinetics, due to a non-trivial molecular rearrangement and resolvation that takes place in every one of the four redox reactions evaluated here, a fact that points towards a probable quasireversible kinetic, a hypothesis that will be further explored in the subsequent sections; besides the fact that they tend to adsorb in the electrode surface, which in turn will also affect the observed kinetics.

Nevertheless, the fact that the RoMWCNT/GC electrode can resolve these four peaks is strong evidence of its improved selectivity towards these compounds. DPV responses using a RoMWCNT/GC electrode in mixtures of different concentrations of AA, DA, UA, and 5HT are shown in Fig. 6a. The peak separation between the four peaks (AA-DA: 132 mV, DA-UA: 130 mV, UA-5HT: 320 mV) allows the selective determination of these four molecules. A linear range was obtained for DA between 5 and 240 μmol L^{-1} ($y = 1.271 + 0.068\ x$. r^2: 0.976) (Fig. 6b) and between 5 and 210 μmol L^{-1} for 5HT ($y = 0.750 + 0.021\ x$. r^2: 0.996) (Fig. 6c), both in presence of AA and UA (Figs. 6d and e).

In DPV, the shape and height of the peaks are criteria for kinetic capabilities of the redox reactions, with high and symmetric peaks corresponding to reversible or quasirevesible kinetics [42,43]. It can be seen that DA and UA present higher peaks, attributable to more favorable kinetics; while AA and 5HT show peaks lower and broader, which means that they present kinetics less favourable. It was mentioned above that the molecular rearrangements during each one of the redox reactions must be taken into account. Hence, DPV results can be seen as evidence for the different extent of the molecular rearrangement involved in each case.

In order to explore quantitatively this hypothesis of molecular rearrangement, kinetical and molecular interpretations were further taken, for each one of the four compounds, based on Tafel´s plot and its equation (the Tafel equation, shown in equation (3), is a special case of the Butler-Volmer model for electrode kinetics, which in turn is derived from the full mathematical treatment of current-potential characteristics, for electrode kinetics).

$$y = (1-\alpha)\, F\, (2{,}303\, RT)^{-1} \qquad (3)$$

where F is the Faraday constant (96.485 kJ mol^{-1}), R is the gas constant (8.314 10^{-3} kJ K^{-1} mol^{-1}), and α the transfer coefficient.

In such cases, a plot of log current vs. overpotential displays a linear region near the half-wave potential where both molecular forms, reduced and oxidised, are present in similar concentrations. The resulting Tafel plots can provide a value for the exchange current density (j_0) from the extrapolated intercept at zero overpotential [42,43]. From j_0 can be easily calculated the value for the standard rate constant (k_0) which is a direct measure of

the kinetic ability of the electrochemical processes, with a higher value that indicates a more favourable electrochemical reaction [43].

According to the extensive literature on the subject [42,43], the chosen region of potential must be the linear section in the plot of log current vs. potential (taken from the positive scan of the voltammetry potential sweep), since non-linear regions are owed to depletion of either reduced or oxidized species and/or mass transfer limitations, which would invalidate the Tafel equation of theoretical electrode kinetics (*i.e*, at very low overpotentials, one of the terms in the Butler-Volmer equation will no longer be negligible and the linearity falls off. At very large overpotentials, mass transfer effects arise and the linearity once again falls off).

The k_0 values obtained for each case are shown in Table 3. They are in very good agreement with the results and interpretations of the preceding CV and DPVs, providing a quantitative explanation for their behaviour. UA and DO have the highest k_0 values, with 5HT showing slower kinetics. It should be reminded that Tafel plots only give linear relationships when the electrochemical process evaluated is not totally reversible. A degree of quasireversibility must be present in order to obtain good Tafel plots, which in turn provides extra criteria for good but not totally reversible kinetics, precisely such as the four compounds examinated in the present work.

Furthermore, Matsuda and Ayabe [44] provide excellent criteria for reversibility in CV, which takes into account the scan rate velocity. For our scan rate (50 mV s^{-1}), the criteria result in:

Reversible kinetics: $k_0 > 1.5\ 10^{-2}$ cm s^{-1}

Quasireversible kinetics: $1.5\ 10^{-2} > k_0 > 10^{-6}$ cm s^{-1}

Totally irreversible kinetics: $k_0 < 10^{-6}$ cm s^{-1}

As can be seen in Table 3, our values for k_0 are in excellent agreement with these criteria, since UA and DO are quasireversible, but have the highest values (and are the most favorable process, as can be seen in both CV and DPV since they show the highest current peaks), while 5HT and AA fall behind in their values, and have lower current peaks in CV and DPV. This quasireversible behaviour, can be possibly explained since the structural changes that take place during the redox reactions examined in this work are not simple electron transfer processes: several changes in bond angles and lengths are inevitably involved, as well as resolvation processes, and those molecular alterations are clearly relevant from an energy point of view [43].

The limit of detection (LOD) was calculated using the formula $3SD\ b^{-1}$, where SD is the standard deviation of 4 consecutive readings of the blank response and b is the slope of the calibration plot of DA or 5HT. LOD for DA was calculated as 235 nmol L^{-1} and 460 nmol L^{-1} for 5HT. These detection limits are higher than other recently reported (Table 4), but many of those reports do not inform the simultaneous determination of DA and 5HT under the presence of AA and UA.

It is extremely important to note that the experiments made in samples with AA, DA, UA and 5HT have been made consecutively, *i.e.* the assays of CV of three samples of different concentrations and DPV of six samples of different concentrations of the four compounds have been measured with the same RoMWCNT/GC modified electrode. These measurements were repeated with three different electrodes (n=3) three different days

under the same experimental conditions to evaluate the inter-electrode reproducibility (Fig. 6f). This fact strongly evidence that the RoMWCN/GC modified electrodes are suitable for the simultaneous determination of DA and 5HT in presence of AA and UA.

4. Conclusions

In this work, an electrochemical treatment has been applied to GC electrodes modified with MWCNT in order to determine in a simultaneous way dopamine (DA) and serotonin (5HT) in presence of ascorbic acid (AA) and uric acid (UA).

Raman spectroscopy revealed that the density of defects increased upon electrochemical treatment but decreased between the oxidation and reduction steps. Thus, despite the fact that our modified electrodes are both functioning as semiconductors, the RoMWCNT/GC electrodes has better conductive properties than the oMWCNT/GC electrodes. The experimental evidence shows that the electrochemical reduction process has restored the sp^2 hybridization. Based on EDS studies, we found a higher amount of atomic percentage of the O element after the electrochemical oxidation process, confirming the oxidation step of MWCNTs, and a reduction of O level after electrochemical reduction, confirming the extent of the reduction step of oMWCNT.

RoMWCNT/GC electrodes present a clear lower R_{CT} when using $Fe(CN)_6^{3-/4-}$ and a lower ΔE_p using $Ru(NH_3)_6^{3+/2+}$ (near the theoretical value of 59 mV) when compared with the other modified electrodes (MWCNT/GC, or oMWCNT/GC). These overall results show that the RoMWCNT/GC electrode facilitated the electron transfer rate, and this might be

attributed to the higher electric conductivity, and a higher electrocatalytic activity of the RoMWCNT/GC, despite the similar calculated ECSA for all the modified electrodes.

SEM images showed fused and unzipped MWCNT in an inner layer, closer to the GC surface electrode, after the oxidation potential treatment applied to a MWCNT/GC; while MWCNT with similar morphology of those found in the untreated MWCNT/GC can be seen in the solution interface of the electrodes.

These modified electrodes may expose different morphologies to a sample, guaranteeing mass transport and, as a consequence, performance enhancement of the electrodes increasing selectivity of DA and 5HT [2,45]. The performance enhancement is reached using RoMWCNT/GC electrodes, given their favourable electrochemical properties evidenced by its high $k°_{eff}$ value. The fact that RoMWCNT/GC can determine four peaks in samples with different concentrations of AA, DA, UA, and 5HT is strong evidence of its improved selectivity towards these compounds.

These results were in very good agreement with the analysis of kinetics made through the Tafel equation providing a quantitative explanation for their behaviour. Although UA and DA present the highest k_0 values, 5HT showed slower kinetics, but still a quasireversible behaviour in RoMWCNT/GC electrodes. These behaviour, can be possibly explained since the structural changes that take place during the redox reactions examined in this work are not simple electron transfer processes: several changes in bond angles and lengths are unavoidable, coupled with the fact that adsorption of biomolecules to the electrodes is always an issue.

To the best of our knowledge we report for the first time modified electrodes, with higher selectivity towards the oxidation of DA and 5HT in presence of UA and AA, with differences between peaks higher than 130 mV, great reproducibility with an RSD of 1.7% for DA and 1.6% for 5HT, and LOD of 235 nmol L^{-1} for DA and 460 nmol L^{-1} for 5HT.

Future work will be focused in the improvement of sensibility of DA and 5HT in order to reach the clinical needs for the determination in urine and/or blood samples. A more detailed characterization of the modified electrodes and the fabrication of a disposable modified electrode, for selective determination of DA and 5HT in presence of different interferences is another of our goals.

Acknowledgments

This work was supported by the University of Buenos Aires (IQUIBICEN-CONICET), the National Council for Scientific and Technological Research (CONICET, PIP 112-200801-00502), and the ANPCyT (Préstamo BID, PICT 2014-3407 and PICT 2014-0402). We also want to thank to Silvia Rodriguez, for editing this manuscript and CONICET Researcher Leonardo Slep for kindly provide us hexaammineruthenium (III) chloride, without his help, the electrochemical characterization of the electrodes with this outer-sphere redox probe would not have been possible.

References

[1] T.V. Magdesieva, P.V. Shvets, O.M. Nikitin, E.A. Obraztsova, F.T. Tuyakova, V.G. Sergeyev, A.R. Khokhlov, A.N. Obraztsov, Electrochemical characterization of mesoporous nanographite films, Carbon 105 (2016) 96-102.

[2] S. Nardecchia, D. Carriazo, M.L. Ferrer, M.C. Gutiérrez, F. del Monte, Three dimensional macroporous architectures and aerogels built of carbon nanotubes and/or graphene: synthesis and applications, Chem. Soc. Rev. 42 (2013) 794-830.

[3] C. Yang, M.E. Denno, P. Pyakurel, B.J. Venton, Recent trends in carbon nanomaterial-based electrochemical sensors for biomolecules: A review, Anal. Chim. Acta. 887 (2015) 17-37.

[4] M. Rahman, S. Beg, M.Z. Ahmad, F. Anwar, V. Kumar, Graphene and its diverse applications in healthcare systems, in: M. Aliofkhazraei, N. Ali, W.I. Milne, C.S. Ozkan, S. Mitura, J.L. Gervasoni (eds), Graphene Science Handbook, Vol. 5, Sec. III, CRC Press Taylor & Francis Group, Florida 2016, p. 399.

[5] A. Pandikumar, G.T.S. How, T.P. See, F.S. Omar, S. Jayabal, K.Z. Kamali, N. Yusoff, A. Jamil, R. Ramaraj, S.A. John, H.N. Lim, N.M. Huang, Graphene and its nanocomposite material based electrochemical sensor platform for dopamine, RSC Adv. 4 (2014) 63296-63323.

[6] T.S. Sreeprasad, V. Berry, How do the electrical properties of graphene change with its functionalization? Small 9 (2013) 341-350.

[7] D.C. Elias, R.R. Nair, T.M.G. Mohiuddin, S.V. Morozov, P. Blake, M.P. Halsall, A.C. Ferrari, D.W. Boukhvalov, M.I. Katsnelson, A.K. Geim, K.S. Novoselov, Control of graphene's properties by reversible hydrogenation: evidence for graphane, Science 323 (2009) 610-613.

[8] D. Wei, Y. Liu, Y. Wang, H. Zhang, L. Huang, G. Yu, Synthesis of N-doped graphene by chemical vapor deposition and its electrical properties, Nano. Lett. 9 (2009) 1752-1758.

[9] N. Mohanty, D. Moore, Z. Xu, T.S. Sreeprasad, A. Nagaraja, A.A. Rodriguez, V. Berry, Nanotomy-based production of transferable and dispersible graphene nanostructures of controlled shape and size, Nat. Commun. 3 (2012) 1-8.

[10] W.S. Hummers, R.E. Offeman, Preparation of graphitic oxide, J. Am. Chem. Soc. 80 (1958) 1339-1339.

[11] K.R. Sharma, Synthesis methods for graphene in: M. Aliofkhazraei, N. Ali, W.I. Milne, C.S. Ozkan, S. Mitura, J.L. Gervasoni (eds.), Graphene Science Handbook, Vol. 1, Sec. I, CRC Press Taylor & Francis Group, Florida 2016, p. 31.

[12] D.V. Kosynkin, A.L. Higginbotham, A. Sinitskii, J.R. Lomeda, A. Dimiev, B.K. Price, J.M. Tour, Longitudinal unzipping of carbon nanotubes to form graphene nanoribbons, Nature 458 (2009) 872-876.

[13] H.L. Guo, X.F. Wang, Q.Y. Qian, F.B. Wang, X.H. Xia, A green approach to the synthesis of graphene nanosheets, ACS Nano 3 (2009) 2653-2659.

[14] D.B. Shinde, J. Debgupta, A. Kushwaha, M. Aslam, V.K. Pillai, Electrochemical unzipping of multi-walled carbon nanotubes for facile synthesis of high-quality graphene nanoribbons, J. Am. Chem. Soc. 133 (2011) 4168-4171.

[15] J.K. Yao, G.G. Jr. Dougherty, R.D. Reddy, M.S. Keshavan, D.M. Montrose, W.R. Matson, S. Rozen, R.R. Krishnan, J. McEvoy, R. Kaddurah-Daouk, Altered interactions of tryptophan metabolites in first-episode neuroleptic-naive patients with schizophrenia, Mol. Psychiatry 15 (2009) 938-953.

[16] J.P. Roiser, A. McLean, A.D. Ogilvie, A.D. Blackwell, D.J. Bamber, I. Goodyer, P.B. Jones, B.J. Sahakian, The subjective and cognitive effects of acute phenylalanine and tyrosine depletion in patients recovered from depression, Neuropsychopharmacol. 30 (2005) 775-785.

[17] H.S. Han, H.K. Lee, J-M. You, H. Jeong, S. Jeon, Electrochemical biosensor for simultaneous determination of dopamine and serotonin based on electrochemically reduced GO-porphyrin, Sens. Actuators B 190 (2014) 886-895.

[18] P. De Deurwaerdère, G. Di Giovanni, Serotonergic modulation of the activity of mesencephalic dopaminergic systems: Therapeutic implications, Prog. Neurobiol. 151 (2017)175-236.

[19] P.T. Kissinger, J.B. Hart, R.N. Adams, Voltammetry in brain tissue - a new neurophysiological measurement, Brain Research 55 (1973) 209-213.

[20] S.R. Ali, R.R. Parajuli, Y. Balogun, Y. Ma, H. He, A non oxidative electrochemical sensor based on a self-doped polyaniline/carbon nanotube composite for sensitive and selective detection of the neurotransmitter dopamine: A review, Sensors 8 (2008) 8423-8452.

[21] D.L. Robinson, A. Hermans, A.T. Seipel, R.M. Wightman, Monitoring rapid chemical communication in the brain, Chem. Rev. 108 (2008) 2554-2584.

[22] K.P. Troyer, M.L. Heien, B.J. Venton, R.M. Wightman, Neurochemistry and electroanalytical probes, Curr. Opin. Chem. Biol. 6 (2002) 696-703.

[23] T-Q. Xu, Q-L. Zhang, J-N. Zheng, Z-Y. Lv, J. Wei, A-J. Wang, J-J. Feng, Simultaneous determination of dopamine and uric acid in the presence of ascorbic acid using Pt nanoparticles supported on reduced graphene oxide, Electrochim. Acta 115 (2014) 109-115.

[24] L. Yang, D. Liu, J. Huang, T. You, Simultaneous determination of dopamine, ascorbic acid and uric acid at electrochemically reduced graphene oxide modified electrode, Sens. Actuators B 193 (2014) 166-172.

[25] S. Qi, B. Zhao, H. Tang, X. Jiang, Determination of ascorbic acid, dopamine, and uric acid by a novel electrochemical sensor based on pristine graphene, Electrochim. Acta 161 (2015) 395-402.

[26] J. Zhou, M. Sheng, X. Jiang, G. Wu, F. Gao, Simultaneous determination of dopamine, serotonin and ascorbic acid at a glassy carbon electrode modified with carbon-spheres, Sensors 13 (2013) 14029-14040.

[27] H. Li, Y. Wang, D. Ye, J. Luo, B. Su, S. Zhang, J. Kong, An electrochemical sensor for simultaneous determination of ascorbic acid, dopamine, uric acid and tryptophan based on MWNTs bridged mesocellular graphene foam nanocomposite, Talanta 127 (2014) 255-261.

[28] H. Filik, A.A. Avan, S. Aydar, Simultaneous detection of ascorbic acid, dopamine, uric acid and tryptophan with Azure A-interlinked multi-walled carbon nanotube/gold nanoparticles composite modified electrode, Arabian J. Chem. 9 (2015) 471-480.

[29] C. Wang, R. Yuan, C. Yaquin, S. Chen, F. Hu, M. Zhang, Simultaneous determination of ascorbic acid, dopamine, uric acid and tryptophan on gold nanoparticles/overoxidized-polyimidazole composite modified glassy carbon electrode, Anal. Chim. Acta 741 (2012) 15-20.

[30] A. Ramachandran, S. Panda, S.K. Yesodha, Physiological level and selective electrochemical sensing of dopamine by a solution processable graphene and its enhanced sensing property in general, Sens. Actuat. B 256 (2018) 488-497.

[31] M. Velicky, K.Y. Tam, R.A.W. Dryfe, On the stability of the silver/silver sulfate reference electrode, Anal. Methods 4 (2012) 1207-1211.

[32] M.D. Hanwell, D.E. Curtis, D.C. Lonie, T. Vandermeersch, E. Zurek, G.R. Hutchison, Avogadro: An advanced semantic chemical editor, visualization, and analysis platform, J. Cheminformatics 4 (2012) 1-33.

[33] S. Pei, H.-M. Cheng, The reduction of graphene oxide, Carbon 50 (2012) 3210-3228

[34] A.V. Krasheninnikov, F. Banhart, Engineering of nanostructured carbon materials with electron or ion beams, Nat. Mater. 6 (2007) 723-733.

[35] D. Yoon, H. Cheong, Raman spectroscopy for characterization of graphene, in: C.S.S.R. Kumar (ed.), Raman Spectroscopy for Nanomaterials Characterization, Ch. 9, Springer, Berlin 2012, p. 191.

[36] R.L. McCreery, Advanced Carbon Electrode Materials for Molecular Electrochemistry, Chem. Rev. 108 (2008) 2646-2687.

[37] D.A.C. Brownson, S.A. Varey, F. Hussain, S.J. Haigh, C.E. Banks, Electrochemical properties of CVD grown pristine graphene: monolayer- vs. quasi-graphene, Nanoscale 6 (2014) 1607-1621.

[38] J. Lu, I. Do, L.T. Drzal, R.M. Worden, I. Lee, Nanometal-decorated exfoliated graphite nanoplatelet based glucose biosensors with high sensitivity and fast response, ACS Nano 2 (2008) 1825-1832.

[39] L. Wang, Y. Yamauchi, Facile synthesis of three-dimensional dendritic platinum nanoelectrocatalyst, Chem. Mater. 21 (2009) 3562-3569.

[40] D.A.C. Brownson, P.J. Kelly, C.E. Banks, In situ electrochemical characterisation of graphene and various carbon-based electrode materials: an internal standard approach, RSC Adv. 5 (2015) 37281-37286.

[41] R.S. Nicholson, Theory and application of cyclic voltammetry for measurement of electrode reaction kinetics, Anal. Chem. 37 (1965) 1351-1355.

[42] A.J. Bard, L.R. Faulkner, Electrochemical Methods, Fundamentals and Applications, Ch. 3, John Wiley & Sons, Texas, 2001.

[43] C.M.A. Brett, A.M. Oliveira Brett, Electrochemistry Principles, Methods, and Applications, Part I, Oxford University Press, Oxford, 1993.

[44] H. Matsuda, Y. Ayabe, The theory of the cathode-ray polarography of Randles-Sevcik, Z. Electrochem. 59 (1955) 494-503.

[45] H.X. Kong, Hybrids of carbon nanotubes and graphene/graphene oxide, Cur. Opin. Solid State Mater. Sci. 17 (2013) 31-37.

Captions to illustrations

Fig. 1. SEM images of modified GC electrodes with MWCNT without any treatment (a), with oMWCNT (b and c), and with RoMWCNT (d, e and f).

Fig. 2. Comparisons of Raman spectra of GC (black), MWCNT/GC (red), oMWCNT/GC (blue) and RoMWCNT/GC (green) (n=2). Ratios I_D/I_G are showed in the inset.

Fig 3. (a) Oxidation CV after 0 h (black), 1 h (red), 2 h (green), 3 h (blue), 4 h (cyan), 5 h (magenta), 6 h (yellow) of the electrochemical oxidation of MWCNT/GC. (b) Reduction CV after 0 h (black), 3 h (blue), and 5 h (magenta), of the electrochemical reduction of oMWCNT/GC in 0.5 mol L^{-1} of H_2SO_4 at 100 mV s^{-1} scan rate. Regions marked with a star indicate the potentials at which the modified GC electrodes have been selectively oxidized or reduced.

Fig. 4. (a) CV of $Fe(CN)_6^{3-/4-}$ in PBS at GC (black), MWCNT/GC (red), oMWCNT/GC (blue), and RoMWCNT/GC electrodes (green). (b) Nyquist plots of $Fe(CN)_6^{3-/4-}$ in PBS at GC (black), MWCNT/GC (red), oMWCNT/GC (blue) and RoMWCNT/GC (green) electrodes. In the inset, the high frequency zone of the Nyquist plots has been magnified. (c) CV of Ru $(NH_3)_6^{2+/3+}$ 1 mmol L^{-1} in KCl 1 mol L^{-1} at GC (black), MWCNT/GC (red), oMWCNT/GC (blue), and RoMWCNT/GC electrodes (green).

Fig. 5. CV at 50 mV s^{-1} using an oMWCNT/GC (in blue) or a MWCNT/GC (in red) in samples containing 350 μmol L^{-1} AA, 25 μmol L^{-1} DA, 85 μmol L^{-1} UA, 30 μmol L^{-1} 5HT (solid line); 980 μmol L^{-1} AA, 100 μmol L^{-1} DA, 360 μmol L^{-1} UA, 100 μmol L^{-1} 5HT (dashed line); or 1100 μmol L^{-1} AA, 240 μmol L^{-1} DA, 600 μmol L^{-1} UA, 220 μmol L^{-1}

5HT (dotted line). In the inset it can be seen a CV at 50 mV s^{-1} using a GC electrode in a sample containing 980 μmol L^{-1} AA, 100 μmol L^{-1} DA, 360 μmol L^{-1} UA, 100 μmol L^{-1} 5HT.

Fig. 6. (a) DPV curves of samples with different concentrations of AA (from 15 to 1100 μmol L^{-1}), DA (from 5 to 240 μmol L^{-1}), UA (from 50 to 600 μmol L^{-1}) and 5HT (from 5 to 220 μmol L^{-1}) using a RoMWCNT/GC electrode (it can be seen in the inset CV corresponding to concentration of curves blue and cyan). Linear responses obtained for DA (b), 5HT (c), AU (d), and AA (e). (f) Inter-electrode reproducibility between three electrodes made the same way in different days.

Table 1

Elemental compositions of the GC modified electrodes determined by EDS (n=3).

	C at%	O at%	S at%
MWCNT/GC	98.1 ± 0.5	1.72 ± 0.21	0.20 ± 0.03
oMWCNT/GC	95.4 ± 0.5	3.89 ± 0.18	0.46 ± 0.01
RoMWCNT/GC	97.7 ± 0.2	2.05 ± 0.12	0.22 ± 0.02

Table 2

Values of ECSA and ΔE_p obtained in the electrochemical characterization using Fe $(CN)_6^{3-/4-}$ or $Ru(NH_3)_6^{2+/3+}$ of GC and modified electrodes. The values of R_{CT} were only calculated using Fe $(CN)_6^{3-/4}$. The relative standard deviation, RSD (in parenthesis), was calculated for all measurements, n=3.

Redox Couple	Electrode	ECSA / cm^2	ΔE_p / mV	R_{CT} /Ω
Inner-sphere Fe $(CN)_6^{3-/4-}$	GC	0.0073 ± 0.0006 (8.2%)	72 ± 7 (9.7%)	2097 ± 676 (32.2%)
	MWCNT/GC	0.087 ± 0.006 (6.9%)	96 ± 9 (9.4%)	146 ± 38 (26%)
	oMWCNT/GC	0.071 ± 0.005 (7%)	103 ± 6 (5.8%)	276 ± 19 (6.9%)
	RoMWCNT/GC	0.080 ± 0.006 (7.5%)	95 ± 1 (1.1%)	73 ± 6 (8.2%)
Outer-sphere $Ru(NH_3)_6^{2+/3+}$	GC	0.0061 ± 0.0005 (8.2%)	68 ± 2 (2.9%)	---
	MWCNT/GC	0.049 ± 0.003 (6.1%)	62 ± 2 (3.2%)	---
	oMWCNT/GC	0.048 ± 0.003 (6.3%)	61.9 ± 1.8 (2.9%)	---
	RoMWCNT/GC	0.051 ± 0.003 (5.9%)	60 ± 1 (1.7%)	---

Table 3

j_0 and k_0 values obtained from Tafel plots made from CV assays, measuring each compound individually, with RoMWCNT/GC electrode at 50 mV s^{-1}.

	AA	DA	UA	5HT
j_0	$2.626\ 10^{-8}$	$1.673\ 10^{-6}$	$1.811\ 10^{-5}$	$7.328\ 10^{-7}$
k_0	3×10^{-6}	1×10^{-3}	6×10^{-3}	4×10^{-4}

Table 4

Comparison of RoMWCNT/GC analytical performance with some modified GC electrodes previously reported.

Electrode	Linear range (μmol L^{-1})				LOD (μmol L^{-1})				Reference
	AA	DA	UA	5HT	AA	DA	UA	5HT	
PG[a]	9-2300	5-710	6-1300	--	6.45	2	4.82	--	[25]
MWCNT/MGF[b]	100-6000	0.3-10	5-100	--	18.28	0.06	0.93	--	[27]
Pt/RGO/GCE[c]	--	5-150	10-130	--	--	0.45	0.70	--	[23]
ERGO/GCE[d]	500-2000	0.5-60	0.5-60	--	200	0.5	0.5	--	[24]
ERGO-P[e]	--	0.1-500	--	0.1-300	--	0.035	--	0.0049	[17]
RoMWCNT/GC	120-1150	5-240	10-600	5-210	6.28	0.235	0.11	0.46	Our work

[a]PG: pristine graphene

[b]MWCNT/MGF: MWNTs bridged mesocellular graphene foam

[c]Pt/RGO/GCE: Pt/reduced graphene oxide modified glassy carbon electrode

[d]ERGO/GCE: glassy carbon electrode modified with electrochemically reduced graphene oxide.

[e]ERGO-P: Electrochemically reduced GO-P (is a GC modified electrode).

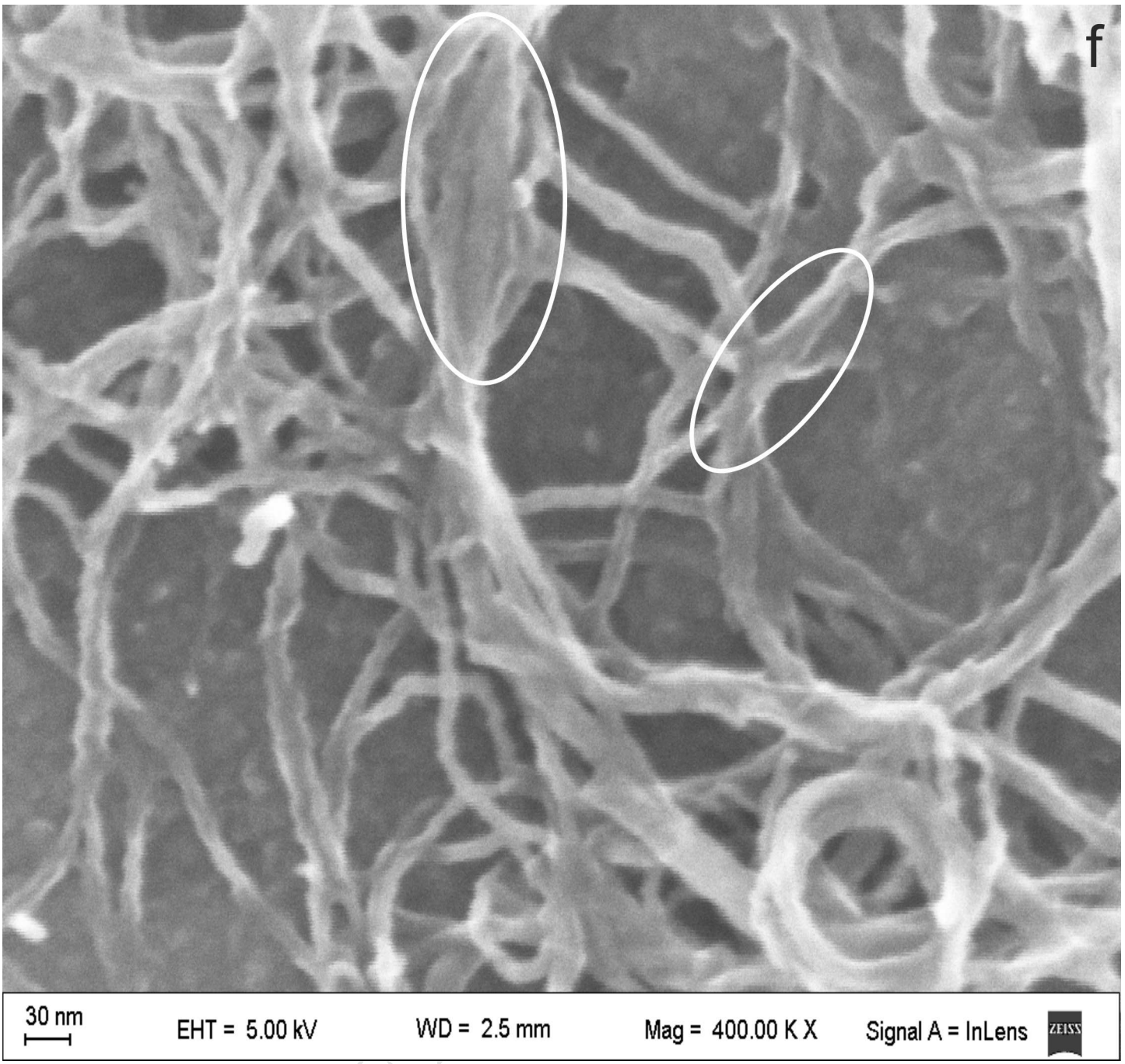

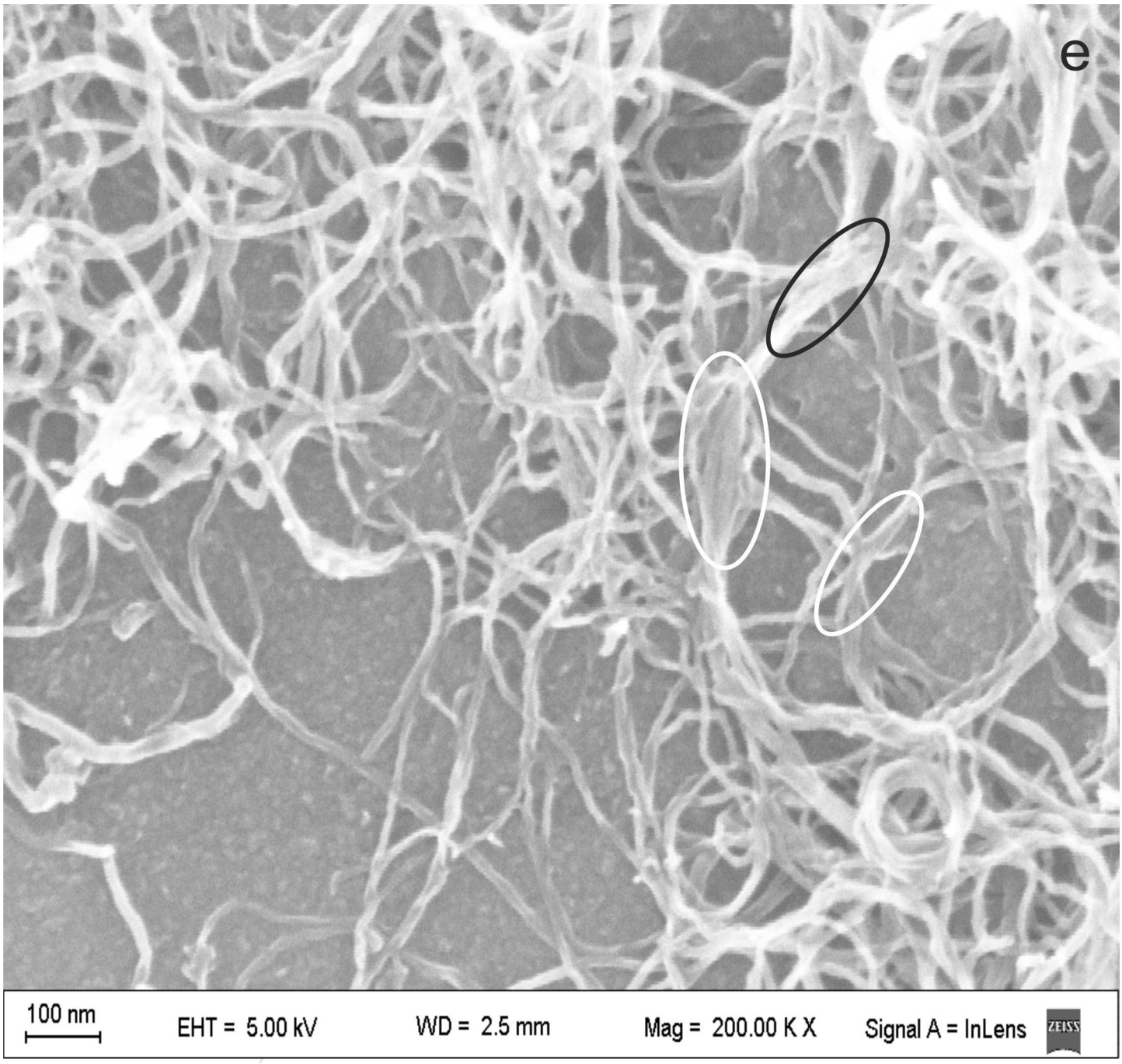
e
100 nm
EHT = 5.00 kV
WD = 2.5 mm
Mag = 200.00 K X
Signal A = InLens
ZEISS

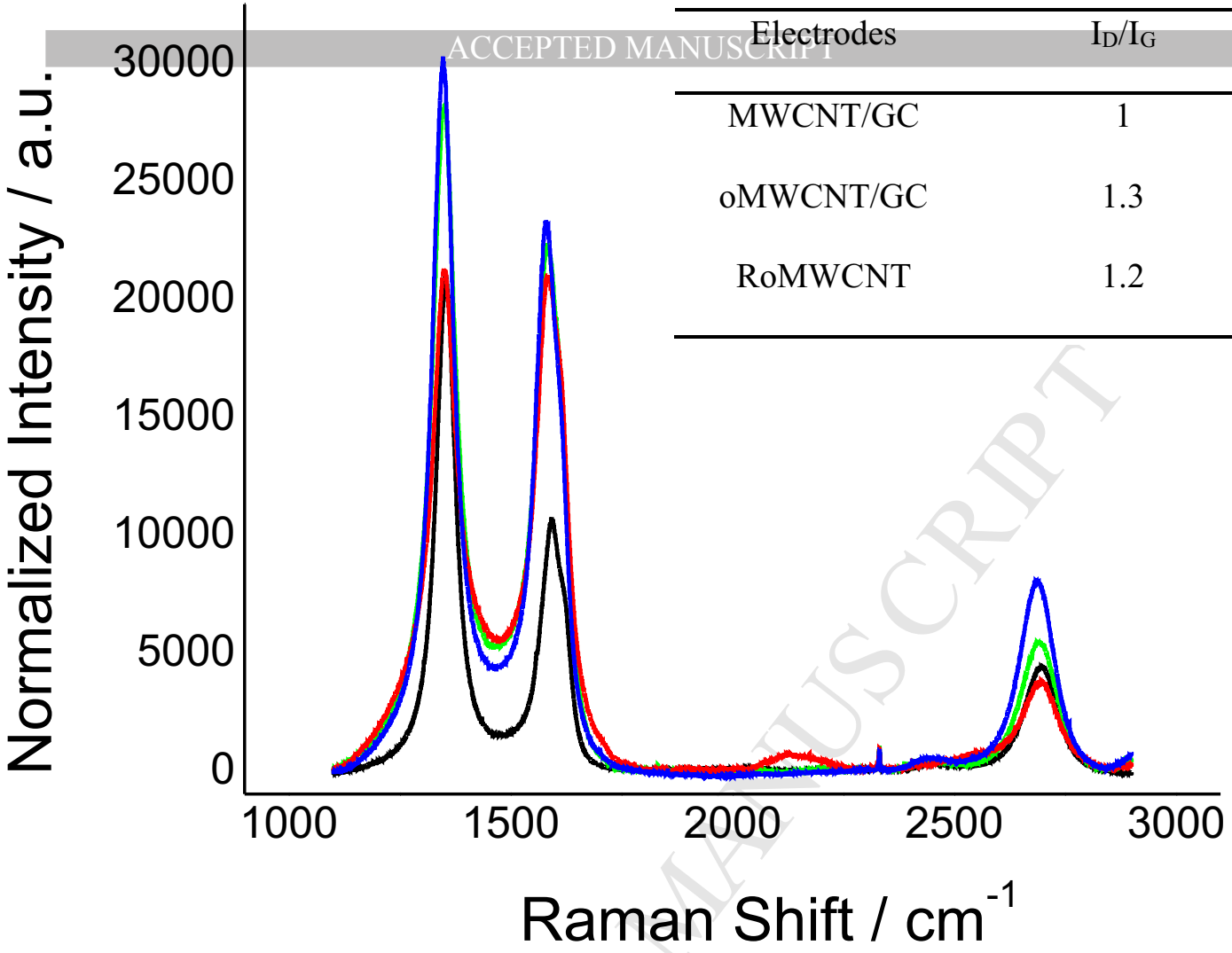

Electrodes	I_D/I_G
MWCNT/GC	1
oMWCNT/GC	1.3
RoMWCNT	1.2

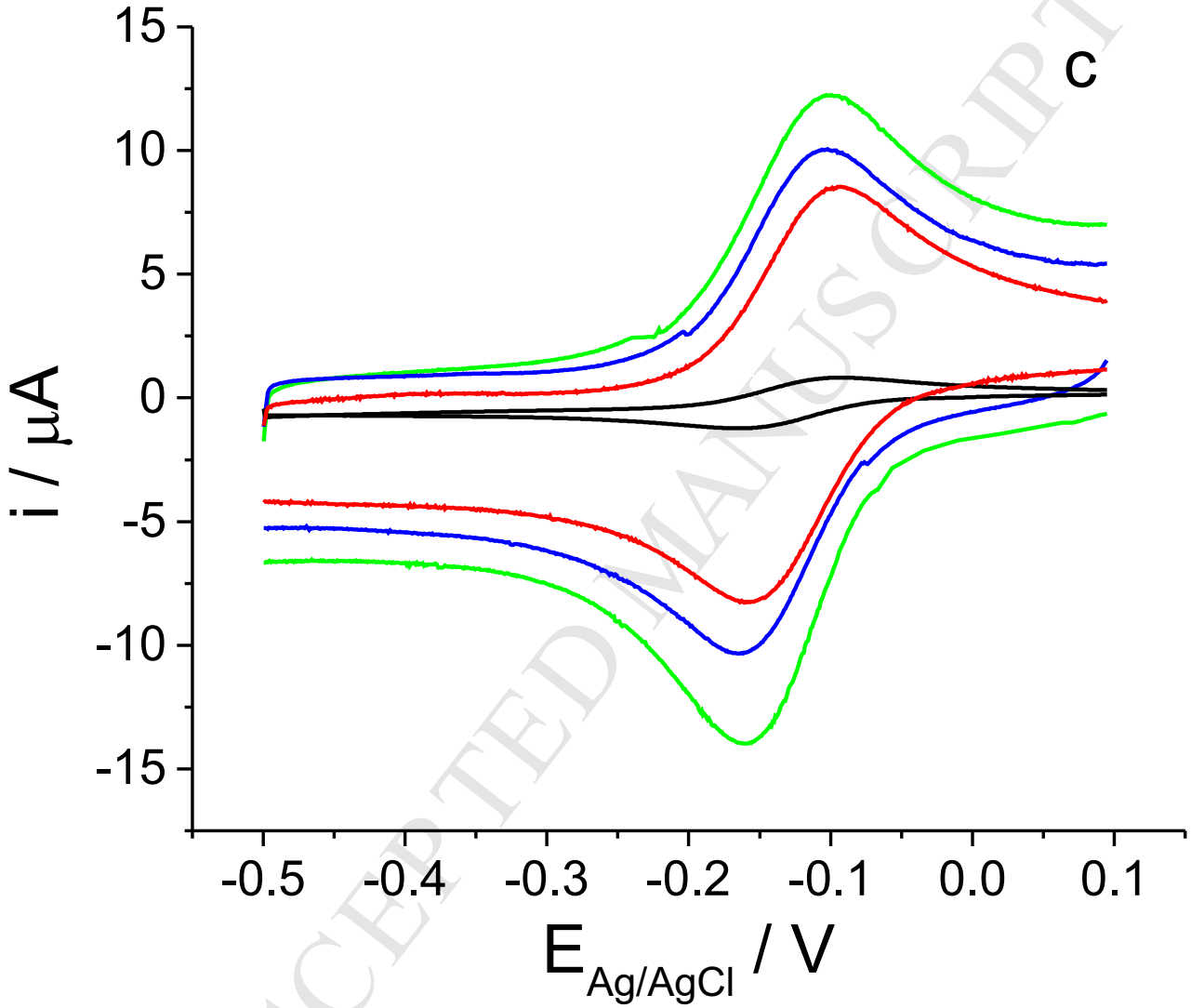

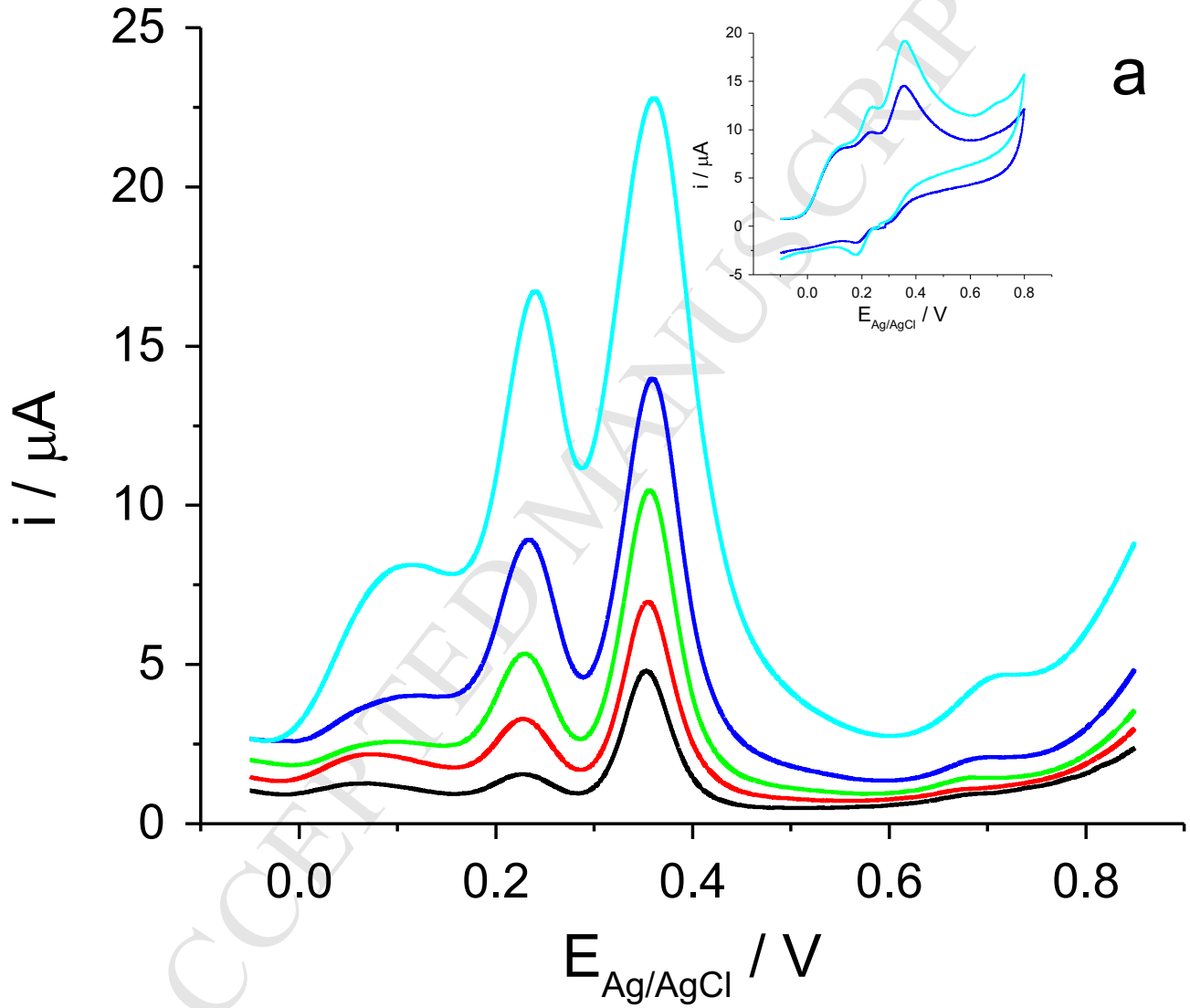

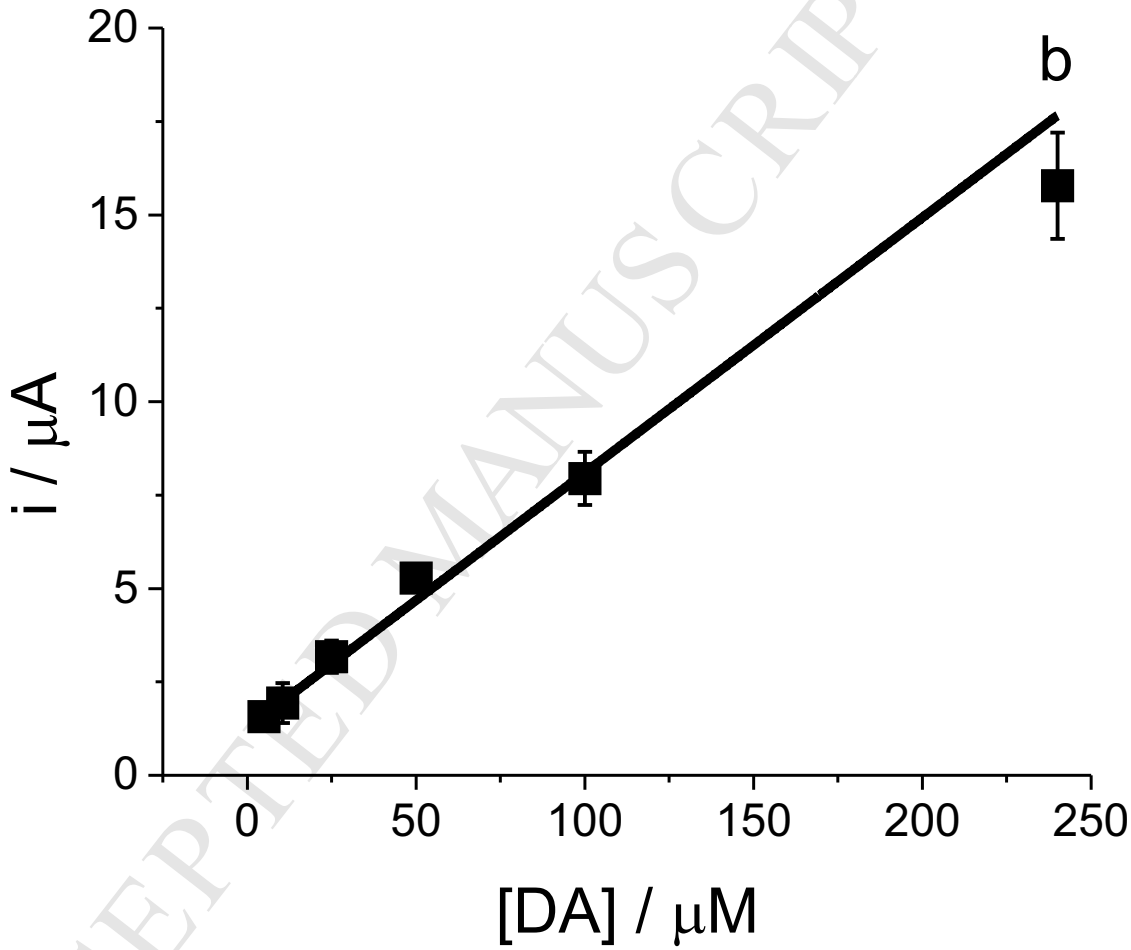

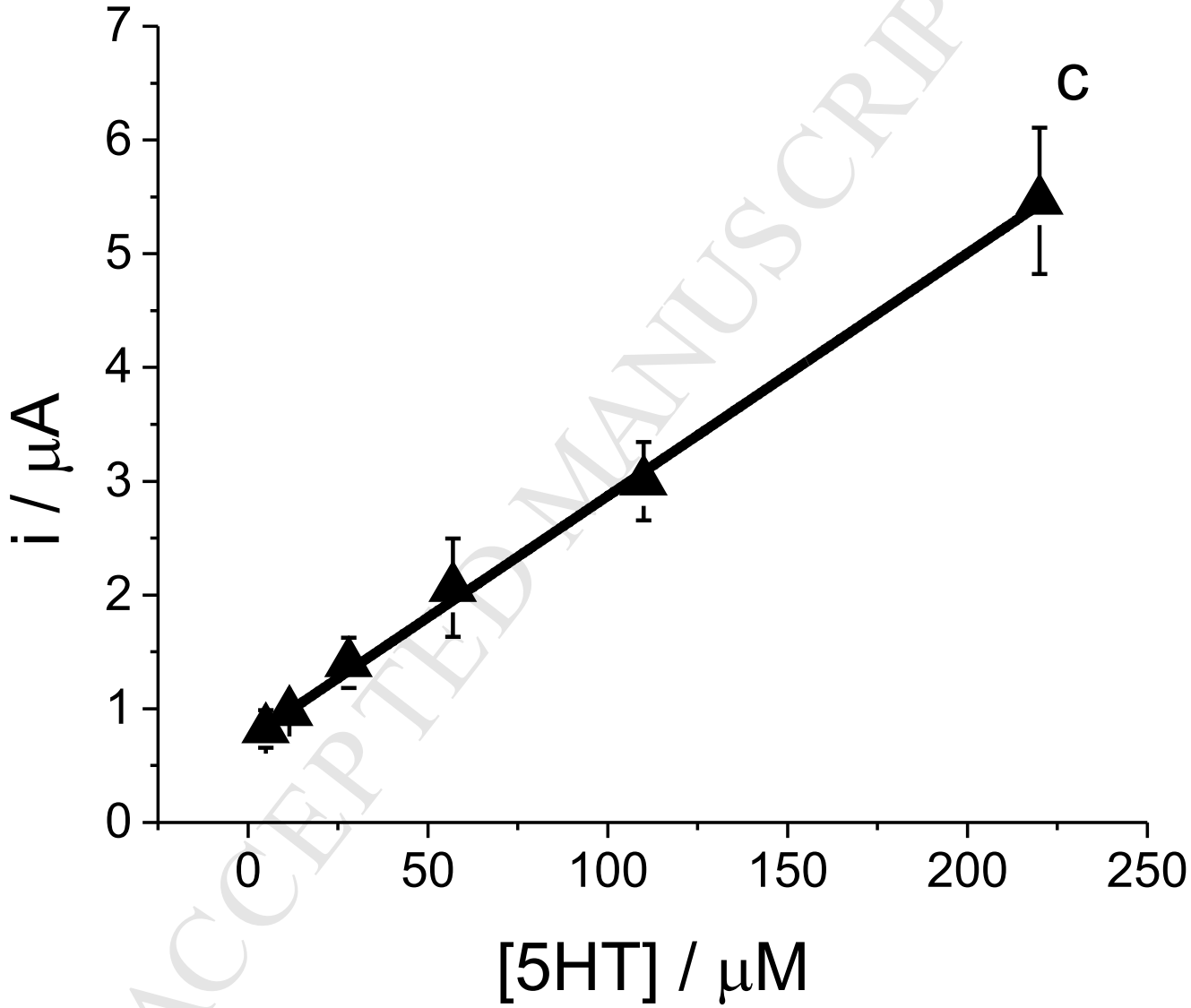

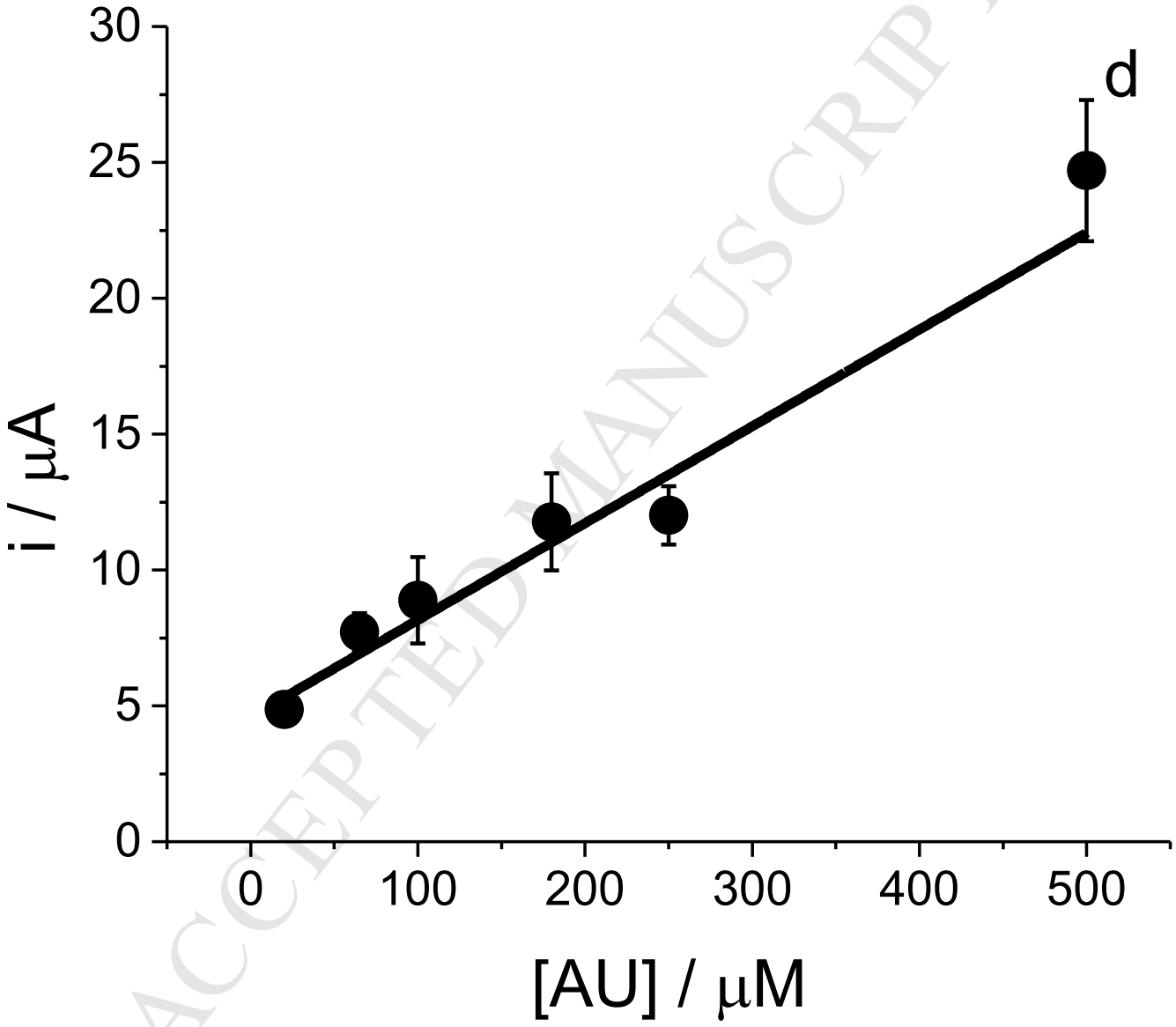

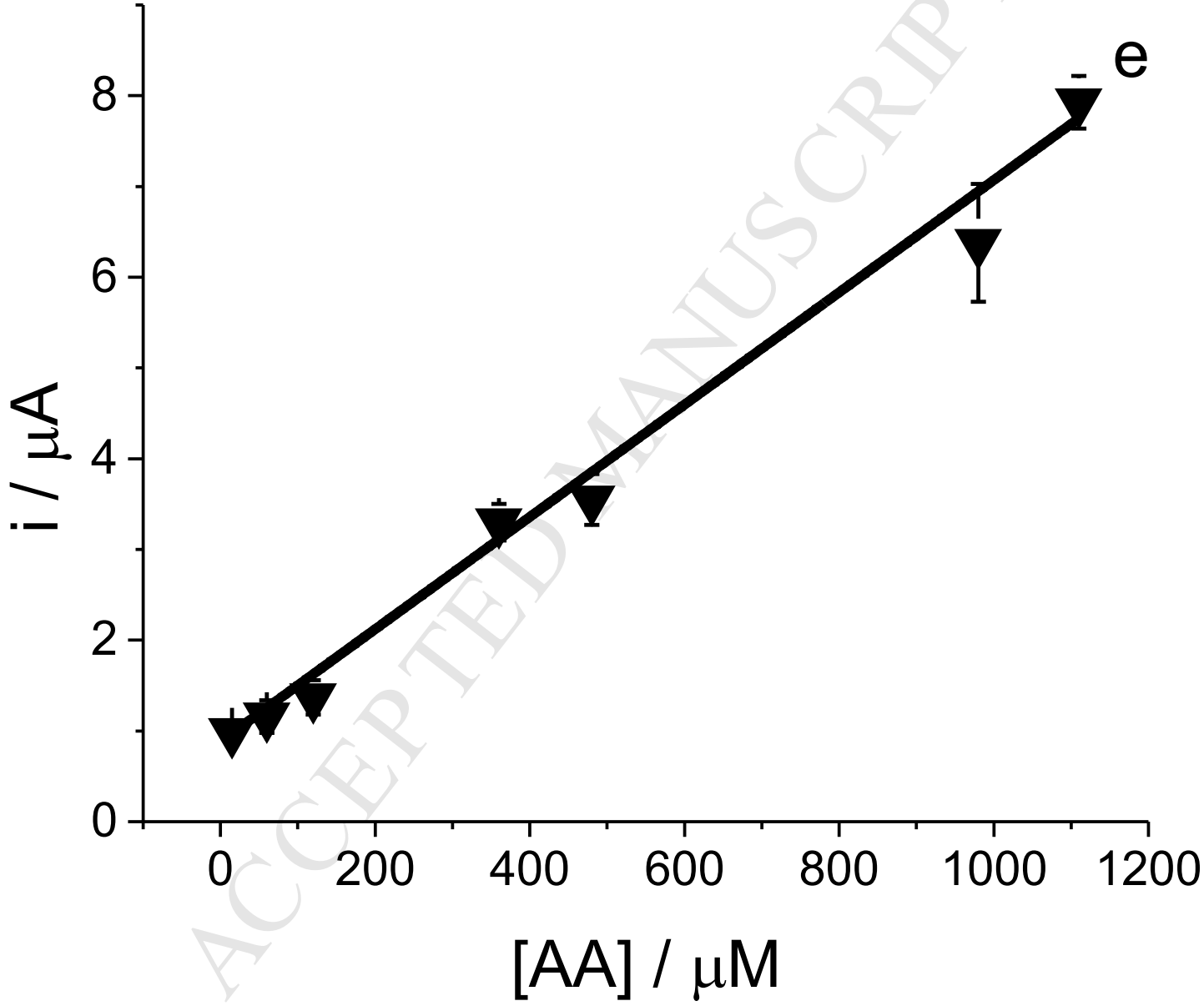

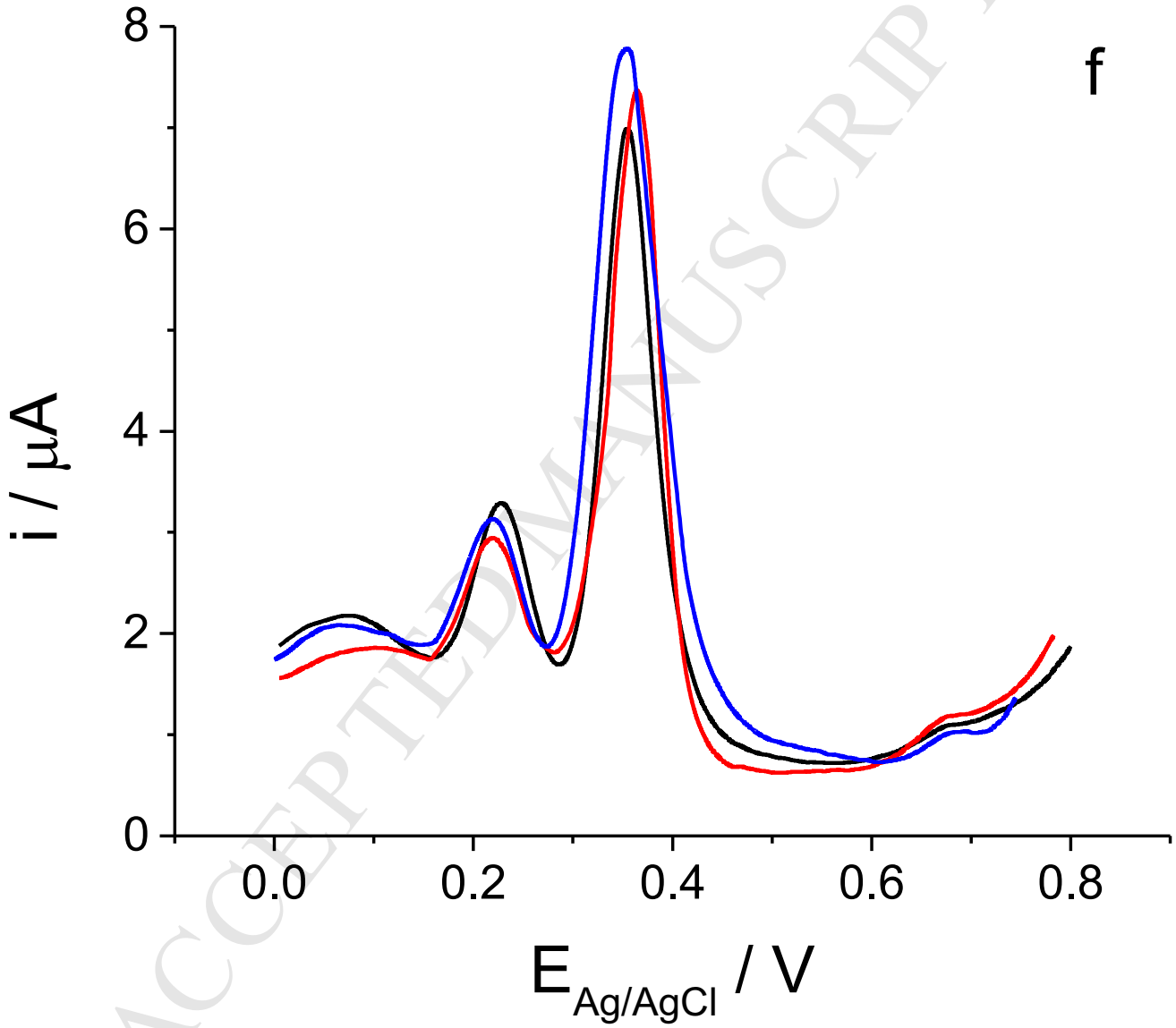

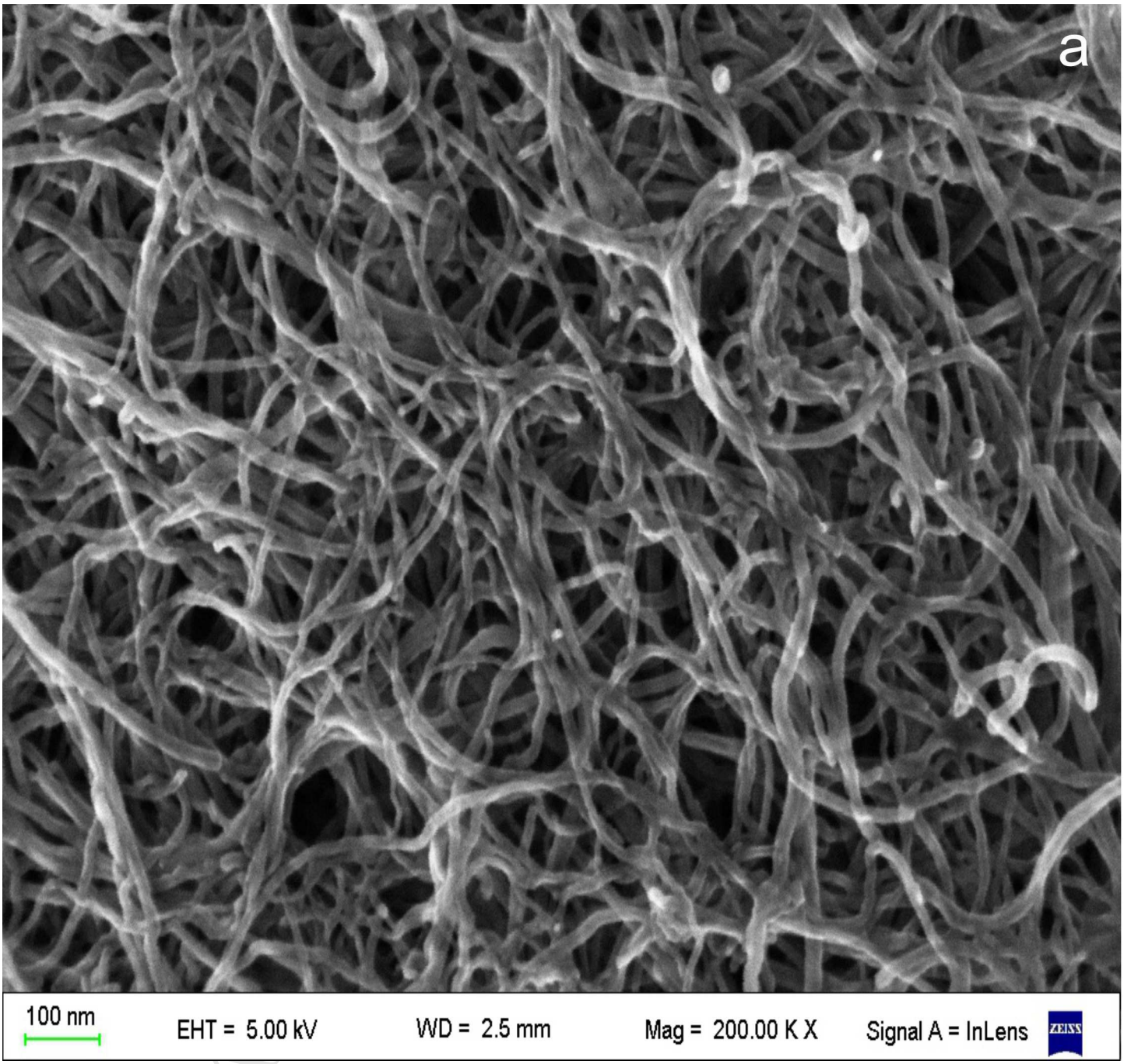
a
100 nm
EHT = 5.00 kV
WD = 2.5 mm
Mag = 200.00 K X
Signal A = InLens
ZEISS

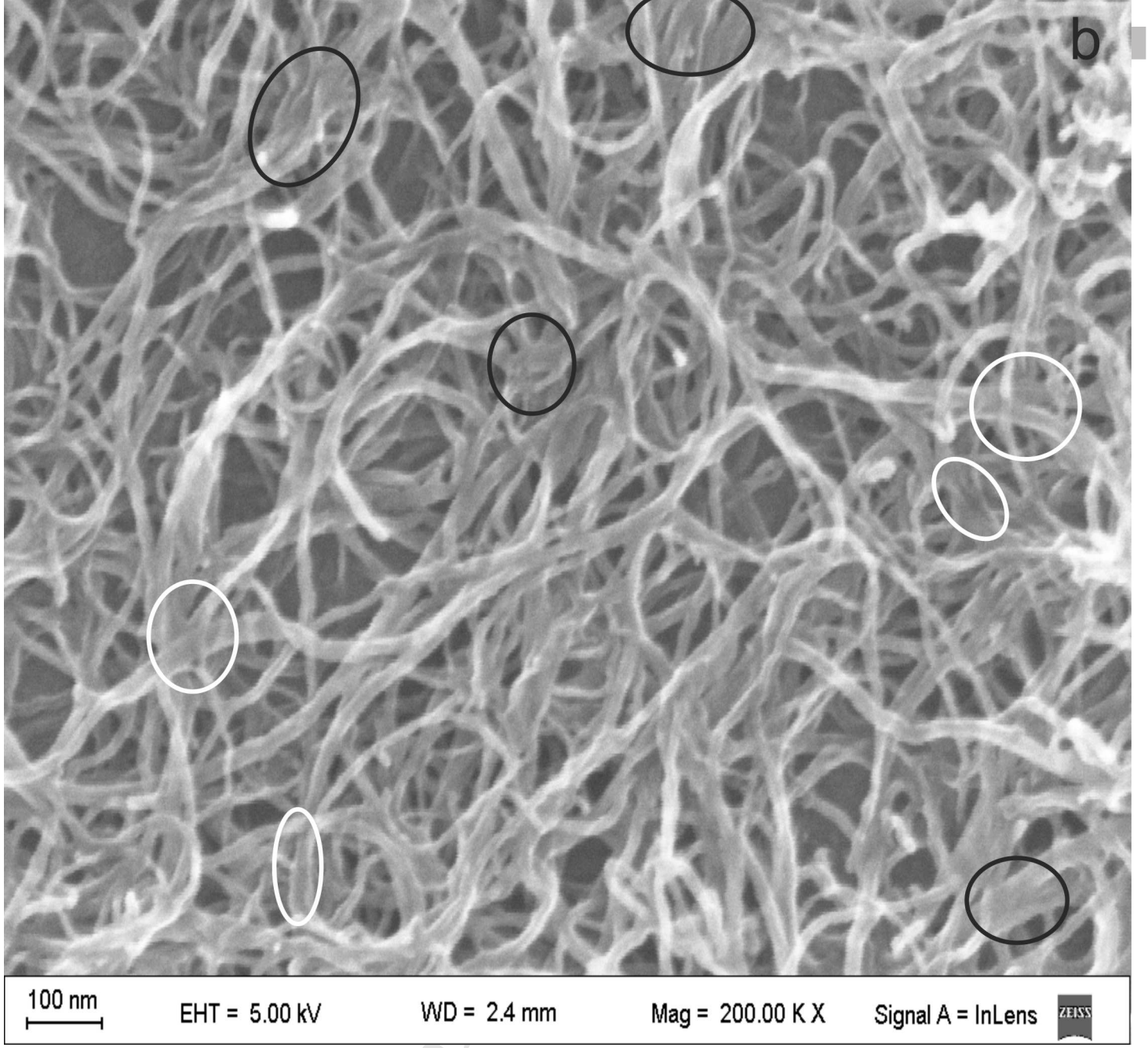

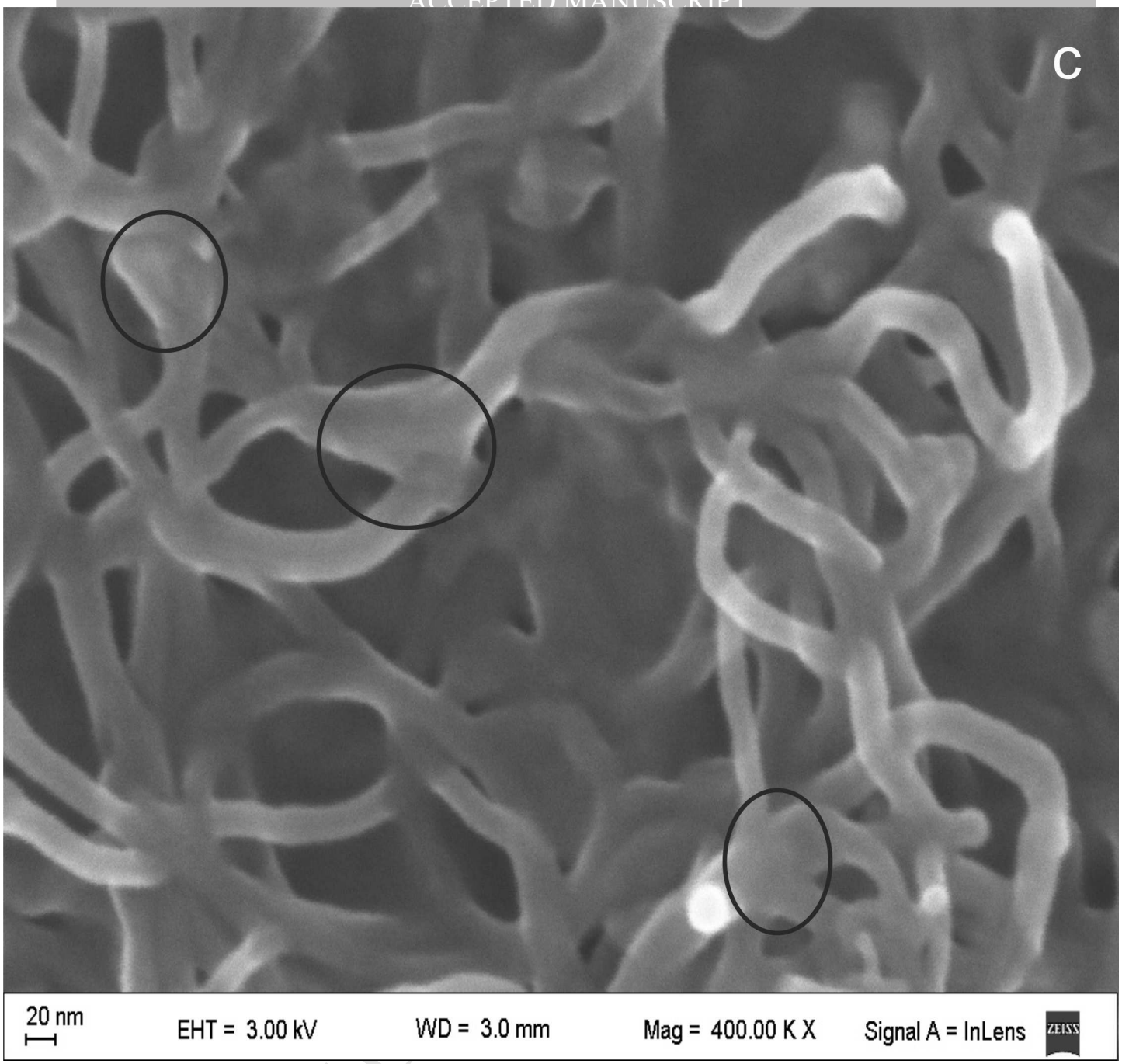

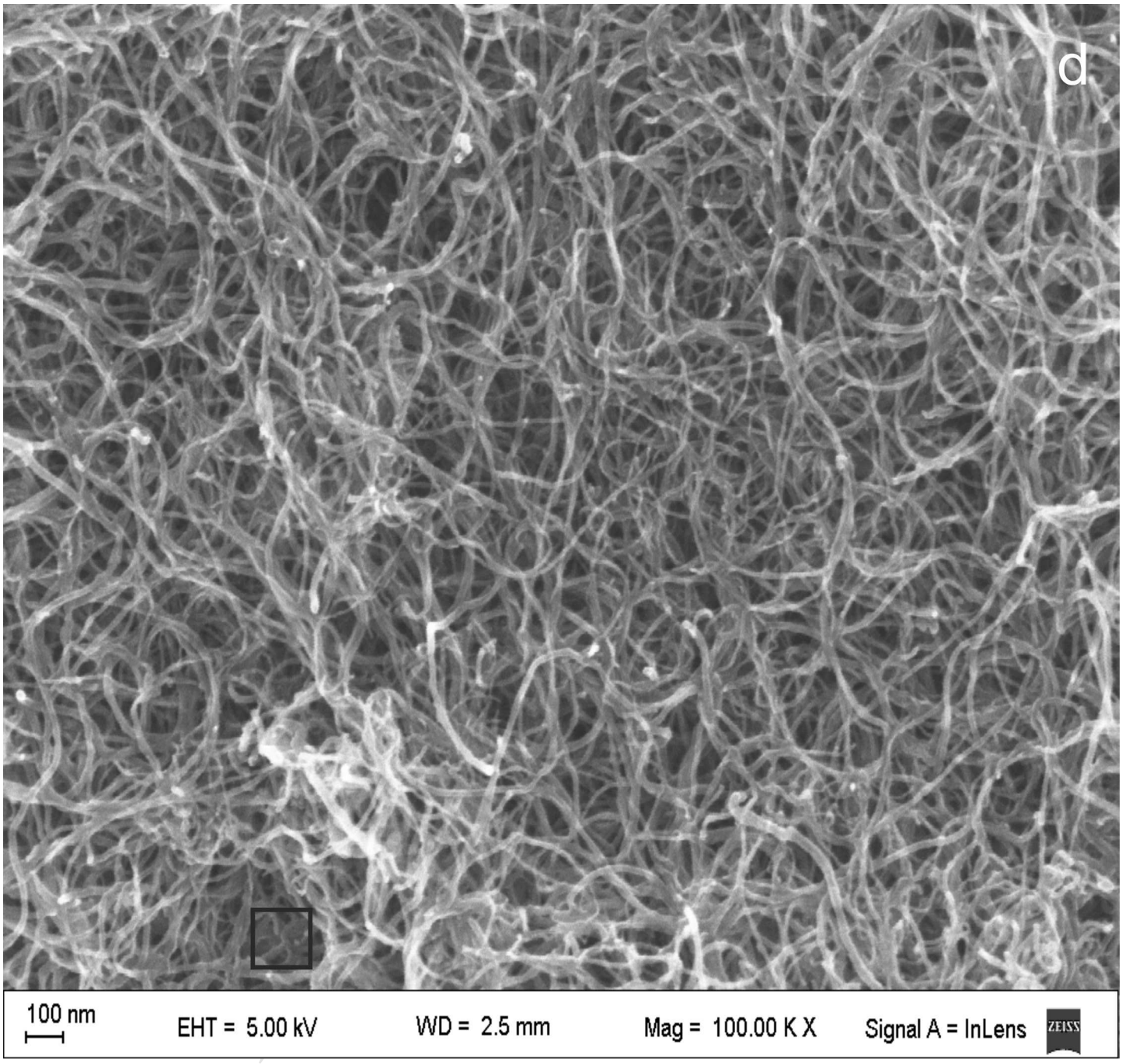
d
100 nm
EHT = 5.00 kV
WD = 2.5 mm
Mag = 100.00 K X
Signal A = InLens
ZEISS

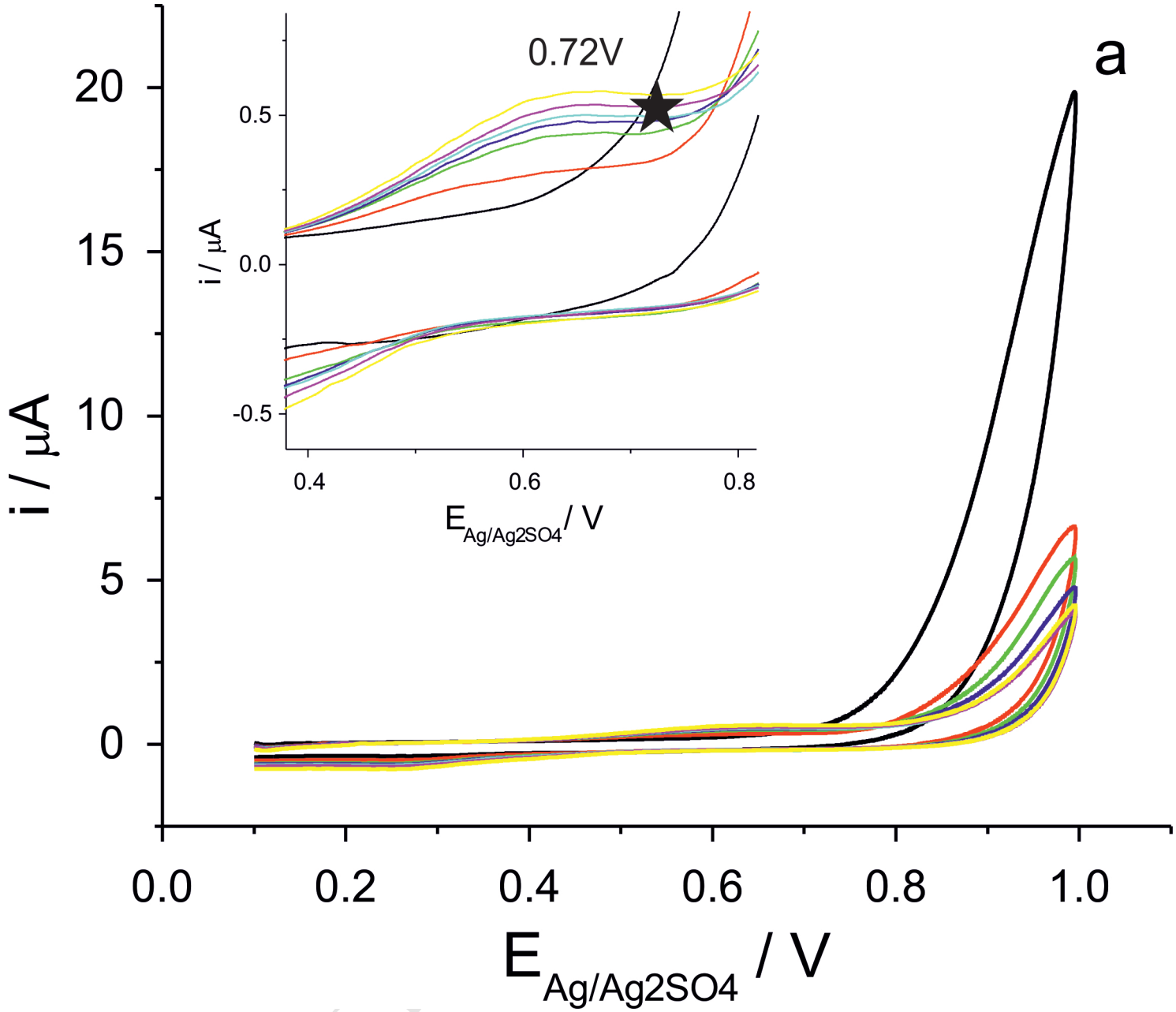
a
0.72V
i / µA
E Ag/Ag2SO4 / V
0.5
0.0
-0.5
0.4
0.6
0.8
20
15
10
5
0
0.0
0.2
0.4
0.6
0.8
1.0

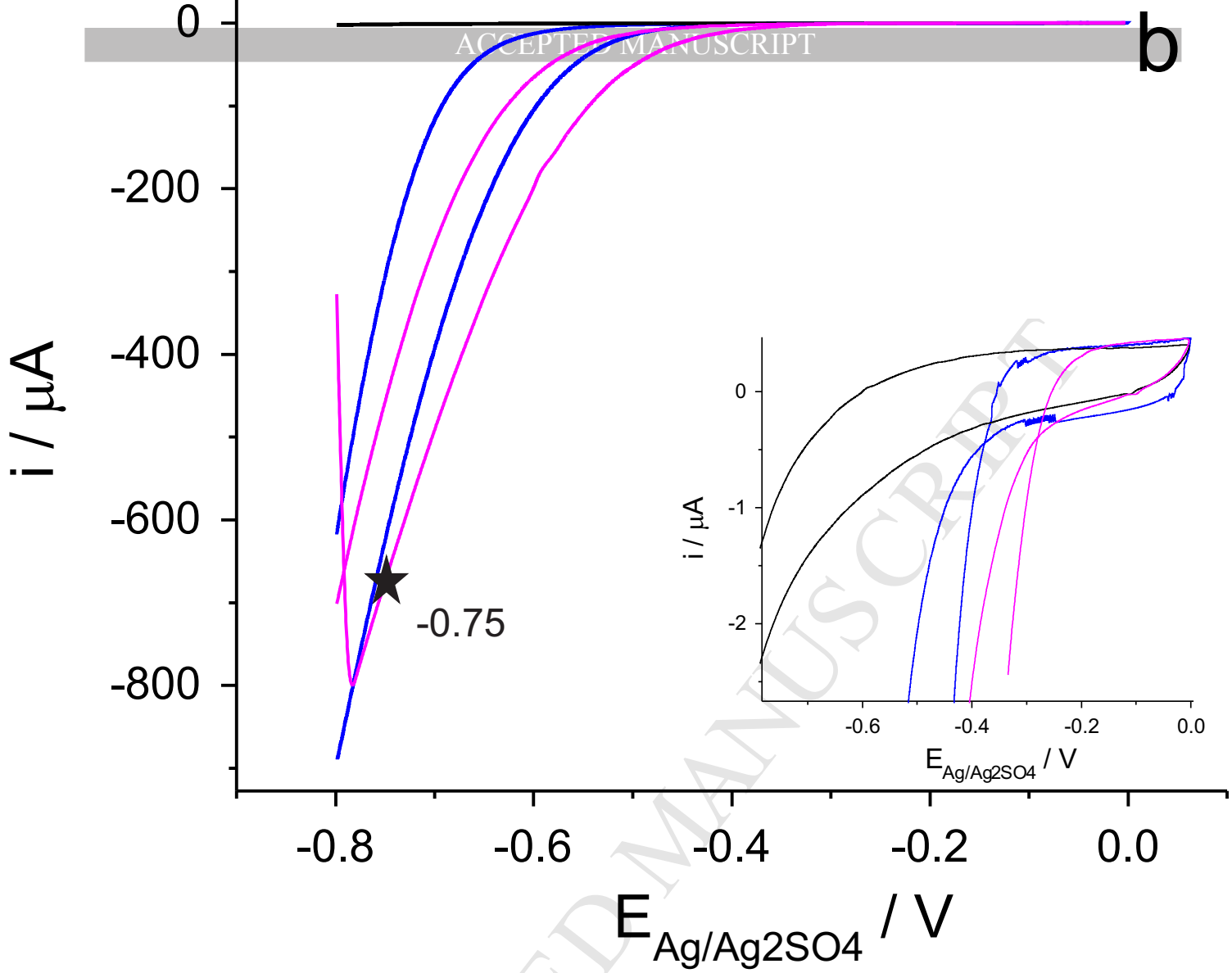

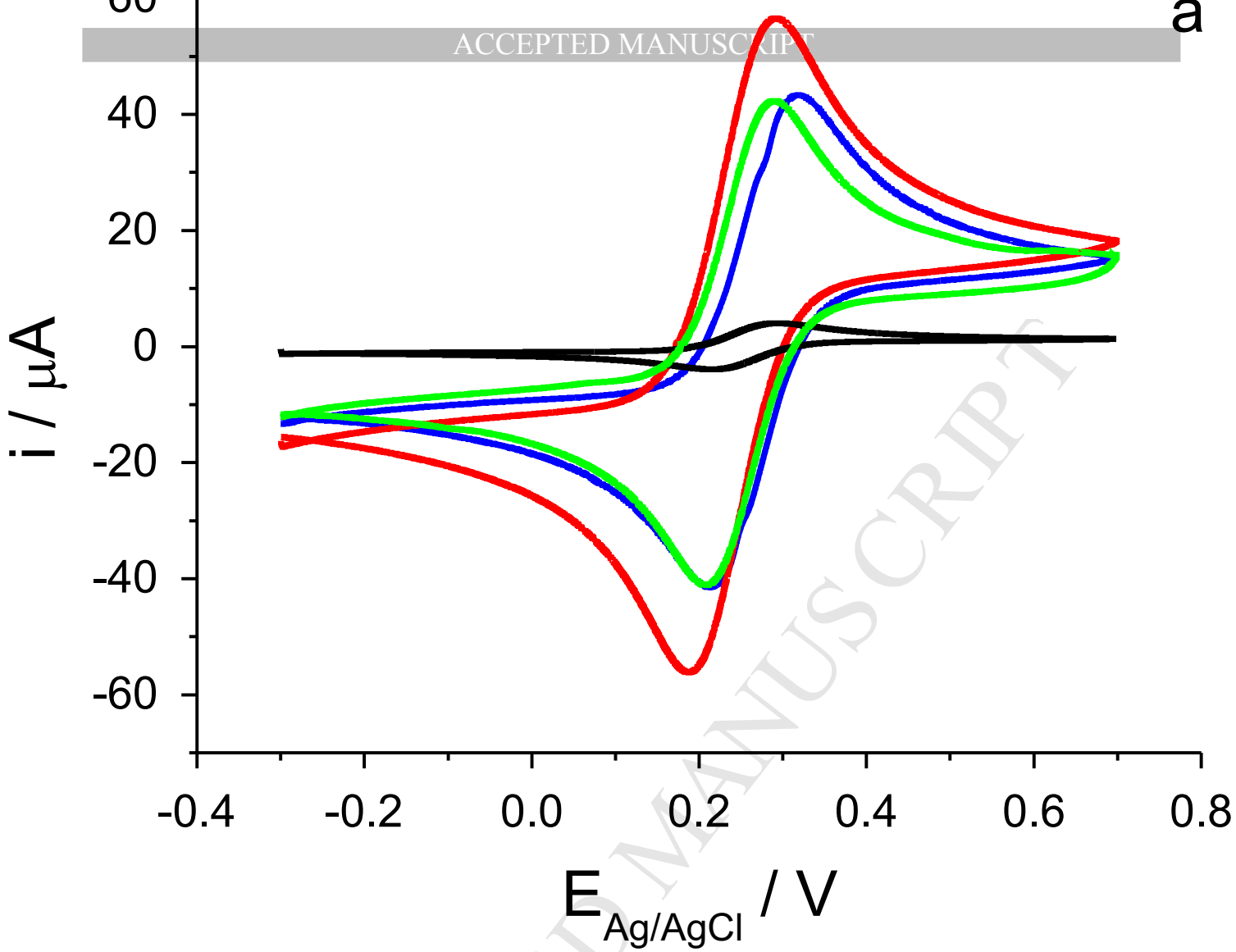

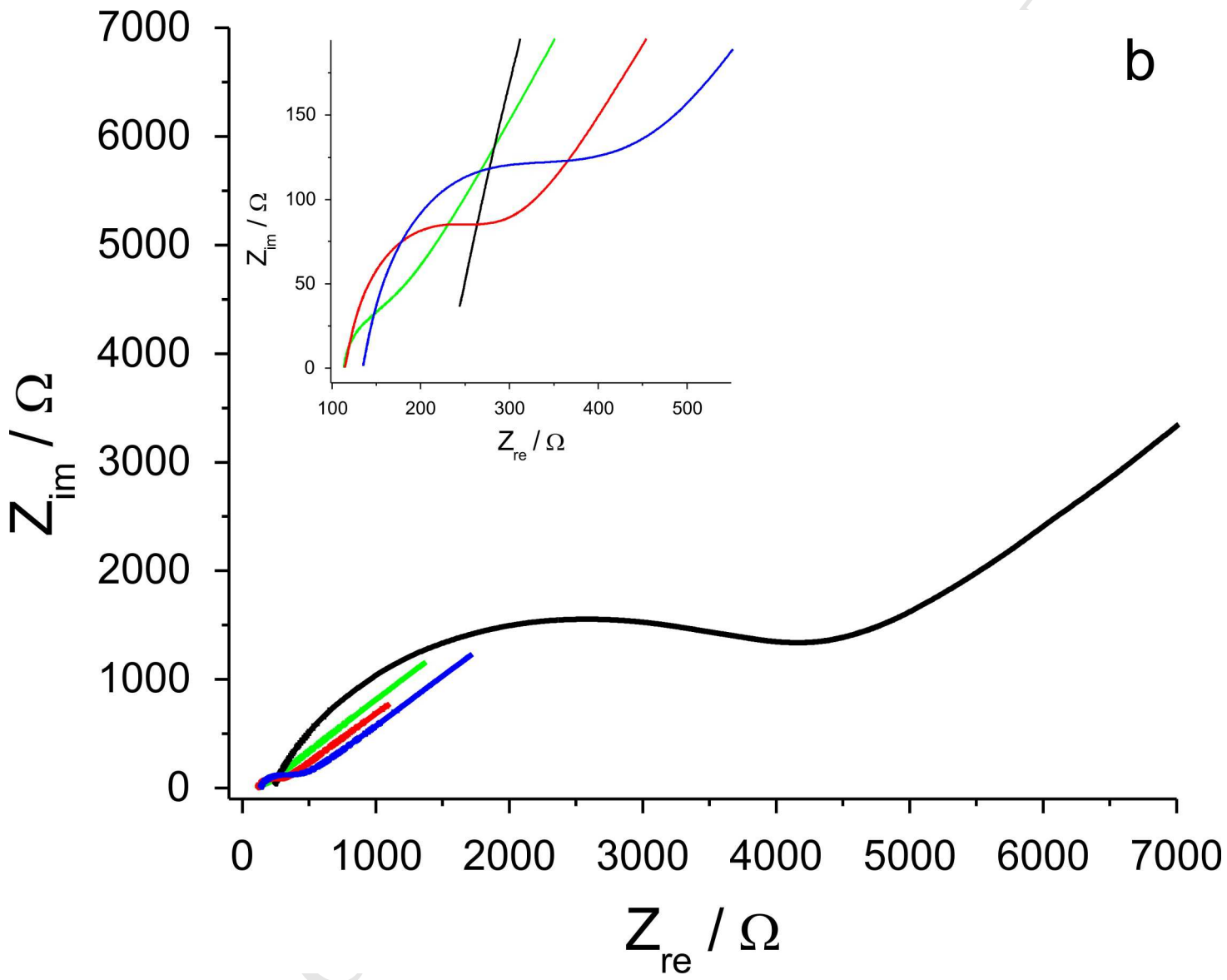
b
7000
6000
5000
4000
3000
2000
1000
0
Z_{im} / Ω
0
1000
2000
3000
4000
5000
6000
7000
Z_{re} / Ω
150
100
50
0
Z_{im} / Ω
100
200
300
400
500
Z_{re} / Ω

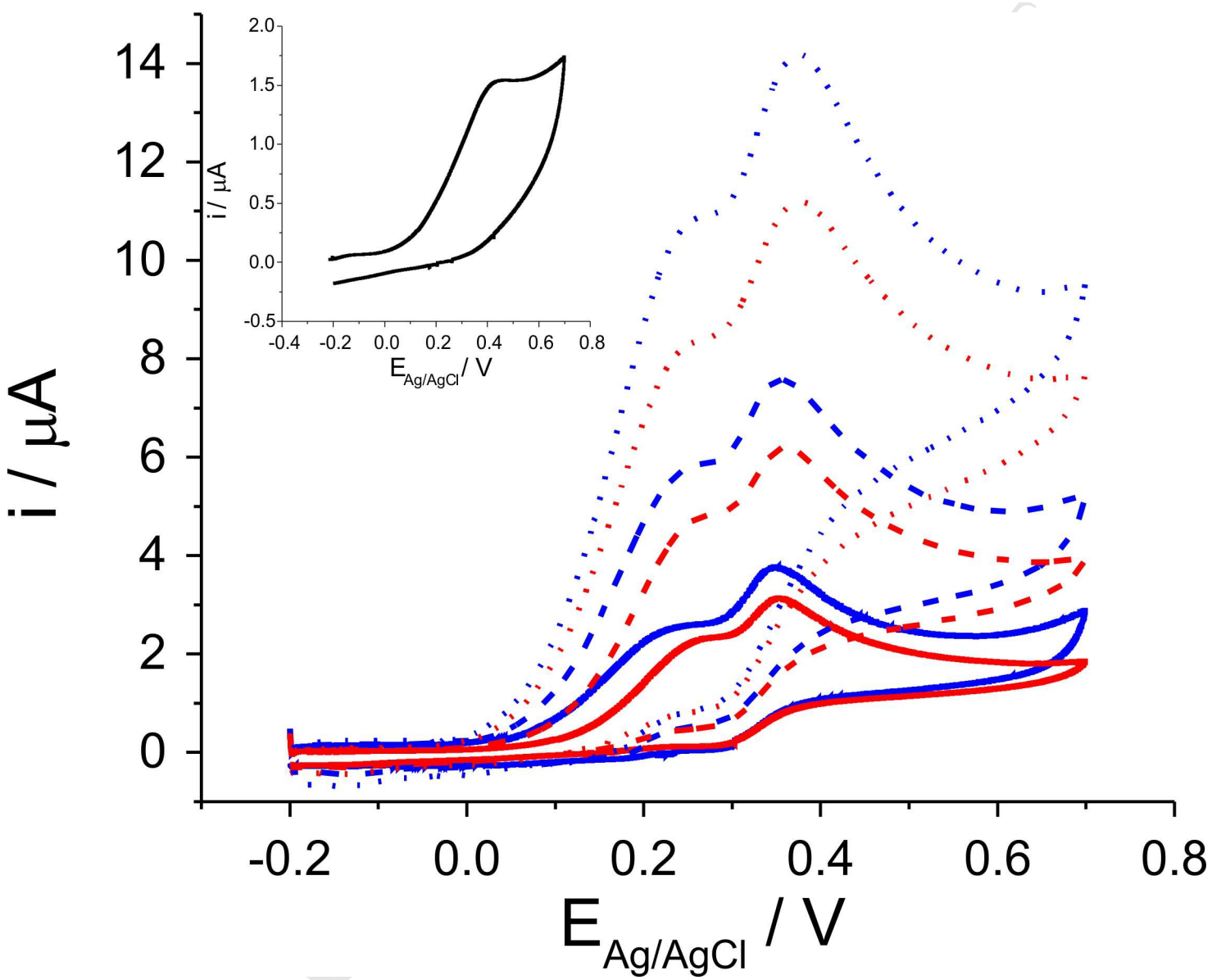
i / µA
14
12
10
8
6
4
2
0
-0.2
0.0
0.2
0.4
0.6
0.8
E Ag/AgCl / V
i / µA
2.0
1.5
1.0
0.5
0.0
-0.5
-0.4
-0.2
0.0
0.2
0.4
0.6
0.8
E Ag/AgCl / V

List of changes:

We have thoroughly revised the manuscript according to the reviewers' suggestions:

We have made new assays using a new batch of $Ru(NH_3)_6^{2+/3+}$ and we have changed Fig 4c, and section 3.5.

We have added values of ECSA of all the electrodes, calculated from using $Ru(NH_3)_6^{3+}$ in, Table 2 calculated.

We have exchanged tables 3 and 4 because they were wrongly numbered according to the order of appearance in the text.

We have highlighted the changes in the revised manuscript.